学　　位　　論　　文

Studies on regeneration therapy for central nervous system using bone marrow stromal cells

（骨髄間質細胞移植による中枢神経再生医療の研究）

2017 年 03 月

北海道大学

譚　成博

Chengbo Tan

学　　位　　論　　文

Studies on regeneration therapy for central nervous system using bone marrow stromal cells

（骨髄間質細胞移植による中枢神経再生医療の研究）

2017 年 03 月

北海道大学

譚　成博

Chengbo Tan

CONTENTS

List of Publications

本研究の一部は以下の論文に発表した。

1. Shichinohe, H., **Tan, C.**, Abumiya, T., Nakayama, N., Kazumata, K., Hokari, M., Houkin, K. & Kuroda, S. Neuroprotective effects of cilostazol are mediated by multiple mechanisms in a mouse model of permanent focal ischemia. Brain Res, 1602, 53-61. 2015

2. **Tan, C.**, Shichinohe, H., Abumiya, T., Nakayama, N., Kazumata, K., Hokari, M., Hamauchi, S. & Houkin, K. Short-, middle- and long-term safety of superparamagnetic iron oxide-labeled allogeneic bone marrow stromal cell transplantation in rat model of lacunar infarction. Neuropathology, 35, 197-208. 2015

3. **Tan, C.**, Shichinohe, H., Wang, Z., Hamauchi, S., Abumiya, T., Nakayama, N., Kazumata, K., Ito, T., Kudo, K., Takamoto, S. & Houkin, K. Feasibility and Efficiency of Human Bone Marrow Stromal Cell Culture with Allogeneic Platelet Lysate-Supplementation for Cell Therapy against Stroke. Stem Cells Int, 2016, 6104780. 2016

4. 王　子澧、**譚　成博**、七戸秀夫、寶金清博
   中国における、中枢神経疾患に対する細胞治療の最新動向。
   再生医療，投稿中

List of Presentations

本研究の一部は以下の学会に発表した。

1. **譚　成博**・七戸秀夫・鐙谷武雄・数又　研・中山若樹・寶金清博
   SPIO でラベリングした骨髄間質細胞、脳梗塞再生医療のソースとしての長期安全性。
   第 13 回日本再生医療学会総会，2014.03・京都

2. 七戸秀夫・鐙谷武雄・中山若樹・数又　研・穂刈正昭・**譚　成博**・寶金清博・黒田　敏
   マウス局所脳虚血モデルに対する、シロスタゾールの ROS 産生抑制作用を介した脳保護効果
   第 15 回日本分子脳神経外科学会，2014.09・山形

3. **Tan, C.**, Shichinohe, H., Abumiya, T., Nakayama, N., Kazumata, K., Hokari, M., Hamauchi, S. & Houkin, K. Short-, middle-, and long-term safety of superparamagnetic iron oxide-labeled allogeneic BMSC transplantation in rat model of lacunar infarction. The 12th International Symposium for Future Drug Discovery and Medical Care, Sep 4-5, 2014, Sapporo, JAPAN.

4. 七戸秀夫・鐙谷武雄・中山若樹・数又　研・穂刈正昭・**譚　成博**・寶金清博・黒田　敏
   シロスタゾールの ROS 産生抑制を介した脳保護作用。
   第 73 回日本脳神経外科学会総会，2014.10・東京

5. **譚　成博**・七戸秀夫・鐙谷武雄・数又　研・中山若樹・寶金清博
   SPIO でラベリングした他家骨髄間質細胞の脳内投与における安全性。
   第 26 回日本脳循環代謝学会総会，2014.11・岡山

6. 七戸秀夫・鐙谷武雄・中山若樹・数又　研・穂刈正昭・**譚　成博**・寶金清博・黒田　敏
マウス局所脳虚血モデルに対する,シロスタゾールの ROS 産生抑制作用を介した脳保護効果。
第 26 回日本脳循環代謝学会総会，2014.11・岡山

7. **譚　成博**・七戸秀夫・濵内祝嗣・鐙谷武雄・数又　研・中山若樹・穂刈正昭・寶金清博
自家骨髄細胞移植による脳梗塞再生医療をめざして：他家ヒト platelet lysate を用いたヒト骨髄間質細胞培養。
第 14 回日本再生医療学会総会，2015.03・横浜

8. 七戸秀夫・**譚　成博**・濵内祝嗣・鐙谷武雄・中山若樹・数又　研・穂刈正昭・寶金清博
脳梗塞に対する自家骨髄間質細胞移植:次世代の再生医療を目指して。
第 14 回日本再生医療学会総会，2015.03・横浜

9. **譚　成博**・王　子澧・七戸秀夫・濵内祝嗣・鐙谷武雄・数又　研・中山若樹・穂刈正昭・寶金清博
ラット脳梗塞モデルにおける全身炎症所見～骨髄間質細胞移植による中枢神経再生治療のために～
第 15 回日本再生医療学会総会，2016.03・大阪

10. 王　子澧・**譚　成博**・七戸秀夫・寶金清博
中国における、中枢神経疾患に対する細胞治療の最新動向。
第 15 回日本再生医療学会総会，2016.03・大阪

11. 七戸秀夫・**譚　成博**・濵内祝嗣・王　子澧・鐙谷武雄・中山若樹・数又　研・寶金清博

脳梗塞に対する自家骨髄間質細胞移植:MSC2.0

第 15 回日本再生医療学会総会，2016.03・大阪

12. 七戸秀夫・**譚　成博**・濵内祝嗣・王　子澧・鐙谷武雄・中山若樹・数又　研・寶金清博

脳梗塞に対する骨髄間質細胞移植：次世代の細胞治療をめざして。

第 41 回日本脳卒中学会総会，2016.04・札幌

13. **Tan, C.**, Wang, Z., Shichinohe, H., Zhao, S., Kuge, Y., Kawabori, M., Abumiya, T., Nakayama, N., Kazumata, K. & Houkin, K. Inflammatory Changes in Brain and Lymphoid Organs after Ischemic Stroke: PET imaging for Cell Therapy. International Stroke Conference 2017, Feb 22-24, 2017, Houston, USA.

14. **譚　成博**・七戸秀夫・王　子澧・川堀真人・久下裕司・東川　桂・趙　松吉・穂刈正昭・寶金清博

PET イメージングによる脳虚血後炎症性変化の評価 : 脳梗塞に対する骨髄間質細胞治療を目指して

第 16 回日本再生医療学会総会，2017.03・仙台

15. 王　子澧・**譚　成博**・七戸秀夫・寶金清博

中国における、中枢神経疾患に対する細胞治療の最新動向。

第 16 回日本再生医療学会総会，2017.03・仙台

List of Abbreviations

AC Number of acquisition

BDNF Brain-derived neurotrophic factor

bFGF Basic fibroblast growth factor

BMSC Bone marrow stromal cell

CNS Central nervous system

CPC Cell processing center

CsA Cyclosporine A

DMEM (Dulbecco's modified Eagle medium)

ELISA Enzyme-linked immunosorbent assay

ES Embryonic stem cell

FCS Fetal calf serum

FDG-PET ^{18}F-fluorodeoxyglucose positron emission tomography

FOV Field of view

GDNF Glial cell line-derived neurotrophic factor

GFP Green fluorescence protein

GMP Good manufacturing practice

GS Gentamicin sulfate

hBMSC (human bone marrow stromal cell)

HE Hematoxylin and Eosin

HGF Hepatocyte growth factor

hPL human platelet lysate

IFN-γ Interferon gamma

IGF-1 Insulin-like growth factor-1

IMZ-SPECT ^{123}I-iomazenil single-photon emission computed tomography

iPS Inducible pluripotent cell

mPL Mixtures of PL

LPS lipopolysaccharide

MRI Magnetic resonance imaging

ND Nondetectable

NGF Nerve growth factor

NSC Neural stem cell

NT Neurotrophin

PBS Phosphate buffered saline

PC Platelet concentrate

PDGF Platelet-derived growth factor

PL Platelet lysate

PRP Platelet-rich plasma

P/S Penicillin/streptomycin

QSM Quantitative susceptibility mapping

RAINBOW The Research on Advanced Intervention using Novel Bone Marrow Stem Cell

sPL Single donor-derived PL

SPIO Superparamagnetic iron oxide

SVZ Subventricular zone

TE Echo time

TGF-β Transforming growth factor-β

TR Repetition time

TSE Transmittable spongiform encephalopathy

VEGF Vascular endothelial growth factor

Preface

Stroke is the second most common cause of death and major cause of disability worldwide[1,2]. According to the World Heart Federation, 15 million people worldwide suffer a stroke each year. Because the limited regenerative capacity of damaged central nervous system (CNS), in these people, nearly six million die and another five million are left permanently disabled in their lifetime though some studies provided a few of treatment options[3]. Recent studies have powerfully suggested that cell transplantation may be a hopeful treatment for stroke. Various cell types have been evaluated as cell source for cell therapy, including embryonic stem (ES) cells, neural stem cells (NSCs), inducible pluripotent cells (iPS) and bone marrow stromal cells (BMSCs) [4-6]. Of these, BMSCs may be the most suitable source of donor cells for humans in clinical situations because they can be harvested from the patients themselves without ethical or immunological problems, and more importantly, they are regarded as no risk of tumorigenesis[7-9].

Bone marrow stromal cells

Bone marrow stromal cells, a kind of mesenchymal stem cells, are multipotent stromal cells that can differentiate into a variety of cell lineages, such as osteoblasts, chondrocytes, myocytes, and adipocytes[10-12]. Since 1998, BMSCs were found the ability to differentiate into neural cells, these cells were regarded as a potential cell source for neural regeneration[13,14].

Recent years, both in vitro and in vivo studies have demonstrated that BMSCs can differentiate into neural cells after transplantation based on the findings of BMSCs' neuron-like morphological change and expression of neuronal phenotype[13-16]. Our study group reported that BMSCs can modify their gene expression profile in response to the surrounding environment[17]. Furthermore, more and more evidence indicated that BMSCs can produce and significantly increase the expression of some neuroprotective and neurotrophic factors, including nerve growth factor (NGF), hepatocyte growth factor (HGF), brain-derived neurotrophic factor (BDNF), neurotrophin (NT)-3, glial cell line-derived neurotrophic factor (GDNF), basic fibroblast growth factor (bFGF), and vascular endothelial growth factor (VEGF), to support the survival of the host neural cells and promote neural functional recovery of patients[18-22,5,23-25].

Although these results are encouraging, several problems still remain unsolved to impede its clinical application.

New generation of cell therapy for stroke: The Research on Advanced Intervention using Novel Bone Marrow Stem Cell (RAINBOW) study

To investigate these unsolved problems and give a new hope for cerebral infarction patients, now our team design a new clinical trial called the RAINBOW study, which is a phase 1 study and uses autologous BMSCs for acute ischemic stroke. In order to avoid the risk of animal product, donor cells will be cultured by allogeneic human platelet lysate (hPL) instead of fetal calf serum (FCS) in cell processing center (CPC). These cells will be labeled with superparamagnetic iron oxide (SPIO) for cell tracking using magnetic resonance imaging (MRI) and then be stereotactically transplanted around the infarct regions. After transplantation, MRI is used for cell tracking, ^{18}F-fluorodeoxyglucose positron emission tomography (FDG-PET) and ^{123}I-iomazenil single-photon emission computed tomography (IMZ-SPECT) are performed for analysis of cellular function, metabolism and therapeutic effects.

Table: Summary of the protocol of the RAINBOW study[26]

Autologous bone marrow stromal cell transplantation for acute ischemic stroke	
Purpose	The primary purpose of the clinical study is to determine the safety of autologous bone marrow stromal cell HUNS001-01 when administered to acute ischemic stroke patients
Phase	Phase 1
Study design	Open label, uncontrolled, dose response study
Condition	Acute ischemic stroke, ICA territory
Intervention	HUNS001-01 will be administered around the infarct area stereotactically. Each patient in one of two groups will be given a dose of 20 or 50 million cells
Primary outcome measures	Safety (time frame: 1 year)
Secondary outcome measures	Improvement in stroke symptoms and functional shift in bio-imaging (time frame: 1 year). Possible improvement in stroke symptoms will be determined by a variety of neurological assessments. Possible functional shift will be assessed using MRI, FDG-PET, and IMZ-SPECT
Estimated enrollment	≥6 (low-dose group: 3, high-dose group 3)

In the present study, we aimed to evaluate the feasibility and the efficacy of hBMSC culture with allogeneic PL (Chapter I), the safety of SPIO-labeled BMSCs and the curative effect of cell therapy after stereotactically transplantation (Chapter II) as the preparatory work for RAINBOW study.

Chapter I

Feasibility and efficiency of human bone marrow stromal cell culture with allogeneic platelet lysate-supplementation for cell therapy against stroke

INTRODUCTION

Human bone marrow stromal cells (hBMSC) have been regarded as a potential cell source for ischemic stroke therapy, owing to their potential to differentiate into multiple cell lineages, their neuroprotective effects, and their ability to promote functional neural recovery of patients[13,27,19,28,24].

Expansion of hBMSCs in *in vitro* culture requires the addition of supplements to the basal culture medium[29]. Fetal calf serum , an expansion supplement isolated from the clotted blood of unborn bovine fetuses, has been commonly added to cell culture mediums because of its high levels of growth stimulatory factors and low levels of growth inhibitory factors[30-33]. Although FCS as a widely accepted standard has been long employed for both research and clinical use, there are increasing safety concerns regarding the use of FCS in clinical-scale cellular preparations due to its xenogeneic origin[34-36]. FCS poses many risk factors, as the administration of animal products to humans may theoretically cause transmittable spongiform encephalopathy (TSE) and zoonoses contamination[37,38]. Moreover, hBMSCs can internalize protein components of FCS and elicit immune reactions in the host when these foreign proteins act as antigenic substrates once transplanted[39,40]. To find for xeno-free agents, cord blood serum, platelet-rich plasma (PRP) and platelet lysate (PL) have been studied as a compelling substitute for FCS[41-43,36].

Platelets play an important role not only in hemostasis but also in wound healing and tissue regeneration[44]. Human PL, obtained by lysing platelet bodies through freeze/thaw cycles, addition of calcium chloride or thrombin activation, is a concentration of various growth factors in human platelets[44]. From 1980, hPL was found to support proliferation of established cell lines, numerous studies have demonstrated that due to the multiplicity of platelet derived growth

factors, hPL is very effective for promoting cell expansion as well as FCS[44,45,37,46,47]. It is known that PL stores a series of potent bioactive mediators including platelet-derived growth factors (PDGF-AA, -AB and -BB), transforming growth factor-β (TGF-β), BDNF, b-FGF, VEGF, insulin-like growth factor-1 (IGF-1), and other important elements[48-50]. These factors have important roles in promoting hBMSC expansion. In addition, PL supplementation doesn't alter the surface markers and multipotent features of the cultured cells compared with those cultured with FCS[51-53].

MATERIALS AND METHODS

Isolation and preparation of PL from human peripheral blood

Nine kinds of platelet concentrates (PC; Lot No. 1, 2, 3, 4, 6, 7, 8, 9, and 10) were collected from nine healthy volunteers by an apheresis system designed for clinical use. The amount of each PC was 10 units in No. 4 and 6, 20 units in No. 8 and 10, and 15 units in others. Freeze/thaw cycles (-150°C/37°C), twice centrifugation with 2000 ×*g* for 20 min and inactivation at 56°C for 30 min were used to produce nine kinds of single donor-derived PLs (sPL). After twice centrifugation with 500 ×*g* for 5 min, these were aliquoted into small portions and frozen at −80°C until being thawed immediately before use[9]. Three kinds of mixtures of PL (mPL) were made from three different sPL (Lot No. 1 + 2 + 3, 4 + 6 + 7, and 8 + 9 + 10).

Measurement of platelet surface antigens and growth factors by enzyme-linked immunosorbent assay (ELISA)

CD41 (human integrin alpha-IIb ELISA kit, CUSABIO, College Park, MD) and CD61 (human integrin beta-3 ELISA kit, CUSABIO) were measured in 12 PL samples (9 sPL and 3 mPL) according to the manufacturer's instructions to speculate on the residual particles of cell membranes. Optical densities were measured by a spectrophotometer (model 550 reader; Bio-Rad, Hercules, CA). All samples and standards were run in triplicate. The growth factor level was extrapolated from a standard curve. If any obtained data were under the mean minimum detectable dose, they were considered as nondetectable (ND) in the analysis.

Concentrations of PDGF-BB (DBB00, R&D Systems, Minneapolis, MN), TGF-β1 (DB100B,

R&D Systems), and BDNF (DBD00, R&D Systems) in 12 PL samples were also measured according to the manufacturer's instructions.

Culture of hBMSCs for cell proliferation assay

Two sources of hBMSCs were adopted in our present study. One was derived from a young donor by purchasing from Cell Applications Inc. (San Diego, CA). According to the manufacture's manual, the ampoule including the frozen cells was thawed, diluted and centrifuged. Pellets were resuspended and plated in 175 cm^2 non-coated flasks (Easy Flask 159910; Nunc, Sigma-Aldrich, St. Louis, MO) with 25 mL of Dulbecco's modified Eagle medium (DMEM)/low glucose (D6046; Sigma-Aldrich) containing 10% preselected FCS (Lot No. 1355888, Gibco, Thermo Fisher Scientific, Waltham, MA) and 1% penicillin/streptomycin (P/S, Sigma-Aldrich). Cells were incubated at 5% CO_2 at 37°C. After 2 or 3 days, non-adherent cells were washed off. The culture medium was replaced 2 or 3 times a week. After the third passage, cells were detached with a 5 min application of 0.05% Trypsin-EDTA (Gibco) at 37°C, counted, and seeded on 6-well plates (6000 cells/well) with FCS-containing DMEM (n = 6) or 12 kinds of 10% PL-supplemented minimum essential medium alpha (αMEM, M0894; Sigma-Aldrich) containing gentamicin sulfate (GS, 40 μg/mL; MSD, Tokyo, Japan), respectively (n = 3 in each PL). After 2 weeks, the cells were counted by an automated cell counter (Invitrogen, Thermo Fisher Scientific).

Isolation and culture of hBMSCs in CPC

The second cell source of hBMSCs was obtained by extracting approximately 50 mL of bone marrow from a healthy volunteer. The bone marrow was brought to CPC of Hokkaido University Hospital, and the following processes were performed in the closed operation system (CPWS system Cell Processing Work Station, Panasonic Healthcare Co., Tokyo, Japan). Bone marrow mononuclear cells were isolated via density-gradient centrifugation with Ficoll-Hypaque (Pharmacia, Uppsala, Sweden), and 1.1×10^7 cells were plated in a 75 cm^2 non-coated flasks (Easy Flask 156499; Nunc) with 15 mL of αMEM with 10% mPL and 40 μg/mL GS. After 48h, non-adherent cells were removed by changing the medium. The culture medium was

replaced 2 or 3 times a week. The hBMSCs were passed three times for the subsequent transplantation.

Cell labeling and collection for MRI tracking

At 24 h before cell injection, 1 μl/ml Ferucarbotran (27.9μg Fe/ml, Resovist®, Fujifilm RI Pharma Co., Ltd., Tokyo, Japan), a SPIO agent, was added into the culture medium to be incubated with BMSCs. SPIO-labeled hBMSCs in flasks were lifted using 4 mL TrypLe Select® (a recombinant trypsin substitute, Gibco) and incubated for 5 min. After fully agitating, cell suspensions were transferred into test tubes and centrifuged at 800 ×*g*, 5 min at 15°C. The supernatant was decanted and the cells were gently resuspended by Artcereb® (the irrigation and perfusion solution for cerebrospinal surgery; Otsuka Pharmaceutical Factory, Inc., Naruto, Japan) to 5×10^7 cells/mL. In order to analyze SPIO-positive hBMSCs, 600 μL/well cell suspensions were seeded on a fibronectin-coated four-well (1.7 cm^2 per well) chamber slide. After 24h, the medium was discarded and the cells on the culture slide were rinsed twice with phosphate buffered saline (PBS). The cells were fixed with 4% acetone for 3 min and then immersed in PBS for 10 min. Subsequently, the slide was stained by Turnbull's Blue method and counted to analyze the concentration of SPIO-labeled hBMSCs.

Flow cytometric analysis

To evaluate the surface markers of hBMSCs, the hBMSCs were suspended and incubated with either a mouse monoclonal antibody against human CD19 (R&D Systems; dilution, 1:100), CD44 (R&D Systems; 1:100), CD45 (R&D Systems; 1:100), CD90 (R&D Systems; 1:100), CD105 (R&D Systems; 1:100), CD106 (R&D Systems; 1:100), CD146 (R&D Systems; 1:100), CD166 (R&D Systems; 1:100), or each mouse isotypic control for 30 min on ice. Cell suspensions were then incubated with Alexa Fluor 488-conjugated secondary antibodies (Molecular Probes, Thermo Fisher Scientific; 1:200) for 30 min on ice. Flow cytometric analysis was performed after two washes using a cytometer (Attune® Acoustic Focusing Cytometer, Applied Biosystems, Thermo Fisher Scientific). Live events (10,000) were acquired for analysis.

Cell injection into decapitated pig brain parenchyma and MR imaging

The SPIO-labelled hBMSCs were stereotactically injected into the striatum of a decapitated pig brain. A burr hole was made 3 cm left of the bregma using a small dental drill. A cell injection needle (Mizuho Co., Tokyo, Japan) attached to a syringe was inserted 4 cm into the brain parenchyma. Then, 300 μL of the cell suspension (5 x 10^4cells/μL) was injected over 5 min. After injection, the needle was left in situ for 5 min to avoid leakage of the injected fluid through the needle tract[54,3].

All MRI data were acquired using a clinical MR scanner (TRILLIUM OVAL, Hitachi, Tokyo, Japan). Quantitative susceptibility mapping (QSM) images were acquired by the use of an RSSG EPI sequence. The sequence parameters were: repetition time (TR) = 30 msec, echo time (TE) = 15 msec, flip angle = 15°, number of acquisition (AC) = 0, matrix = 512 x 512, slice thickness = 1.2 mm.

Histological analysis

The day after cell injection, the pig's brain was removed from the skull and stored in 4% paraformaldehyde for one week. It was then sliced and embedded in Tissue Freezing Medium O.C.T. Compound (Sakura Finetek Japan Co., Ltd., Tokyo, Japan), and quickly frozen in liquid nitrogen. Frozen sections of 12 μm thickness were mounted on silane-coated glass slides. During Turnbull's blue analysis, sections were dipped into 10% ammonium sulfide solution (Sigma-Aldrich) overnight, followed by incubation with compound solution mixed in 20% potassium ferricyanide (Wako, Osaka, Japan) and 1% HCL solution for 20 min. Nuclear fast red solution was used for counterstaining.

For fluorescent immunohistochemistry, after blocking non-specific reactions, sections were treated with a mouse anti-human nuclei monoclonal antibody MAB1281 (1:100 dilution) as the primary antibody at 4°C overnight followed by incubation with Alexa Fluor 594 Goat Anti-mouse IgG (H+L) Antibody (1:200, Life Technologies, Thermo Fisher Scientific) as the secondary antibody at room temperature for 1h. The fluorescence emitted was observed through each appropriate filter on a fluorescence microscope (BX51, Olympus, Tokyo, Japan) and was digitally photographed using a cooled CCD camera (model VB-6000/6010, Keyence, Japan).

RESULT

Residues of cell membrane in PL

ELISA analysis demonstrated that the platelet cell surface antigen CD41 of all PL samples was not detected (the lower limitation of detect range: 156 pg/mL). CD61 was detected in the all samples, however, the mean amount was extremely small (210 ± 63 pg/mL; mean ± SD, Fig. 1A).

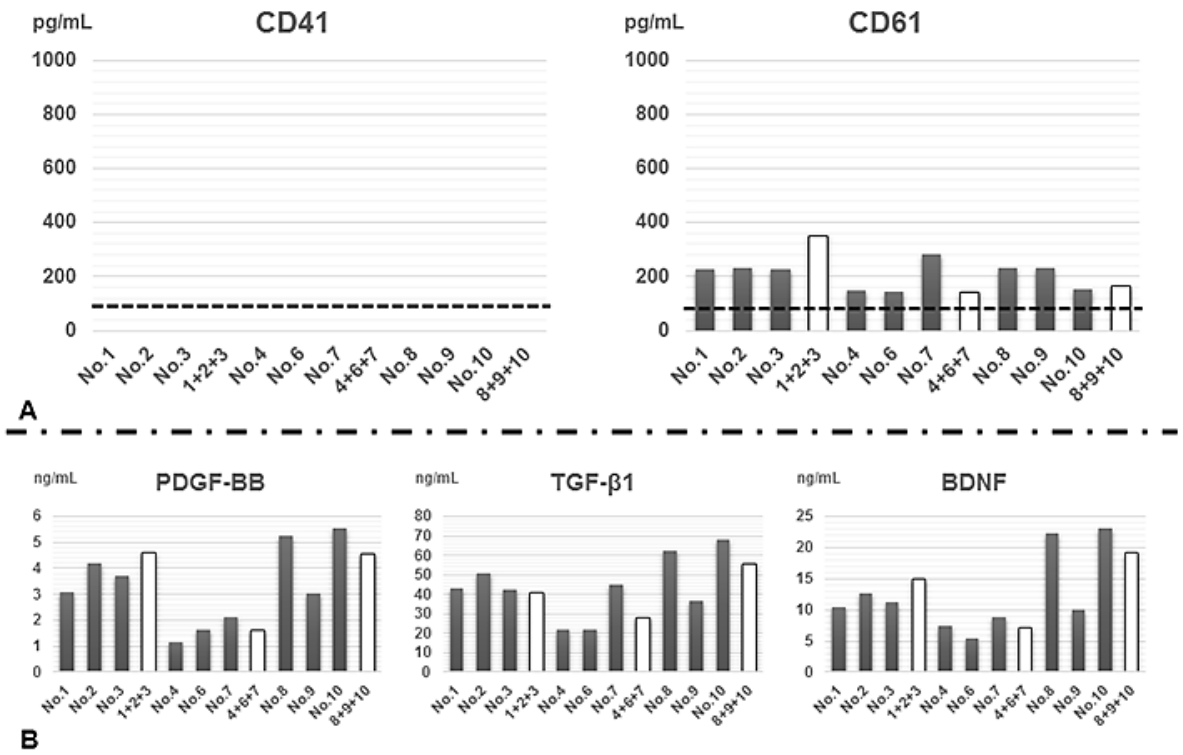

Figure 1: Panel A shows ELISA analysis for cell surface antigens of platelets (left: CD41, right: CD61). The broken lines indicate each mean minimum detectable dose. Panel B shows the measurement of growth factors in PL samples. Each graph indicates the concentration of human PDGF-BB, TGF-β1, and BDNF in the 12 kinds of fresh PL samples, respectively. Gray bars: sPL), white bars: mPL.

Growth factors contained in PL

The mean concentrations of human PDGF-BB, TGF-β1, and BDNF were 3.36 ± 2.20 ng/mL, 44.9 ± 23.0 ng/mL, and 14.3 ± 8.9 ng/mL in all PL samples, respectively (Fig. 1B). The concentration in each PL seemed to be correlated among the growth factors and there was a big difference among each sample, especially sPL, for every growth factor. When the data were analyzed for the platelet units in original PC, we found that the amount of these growth factors

correlated with platelet units in original PC (Fig. 3A). Among mPL, there was a relatively small difference in concentrations because they were balanced by mixtures of 3 different sPL (Fig. 1B).

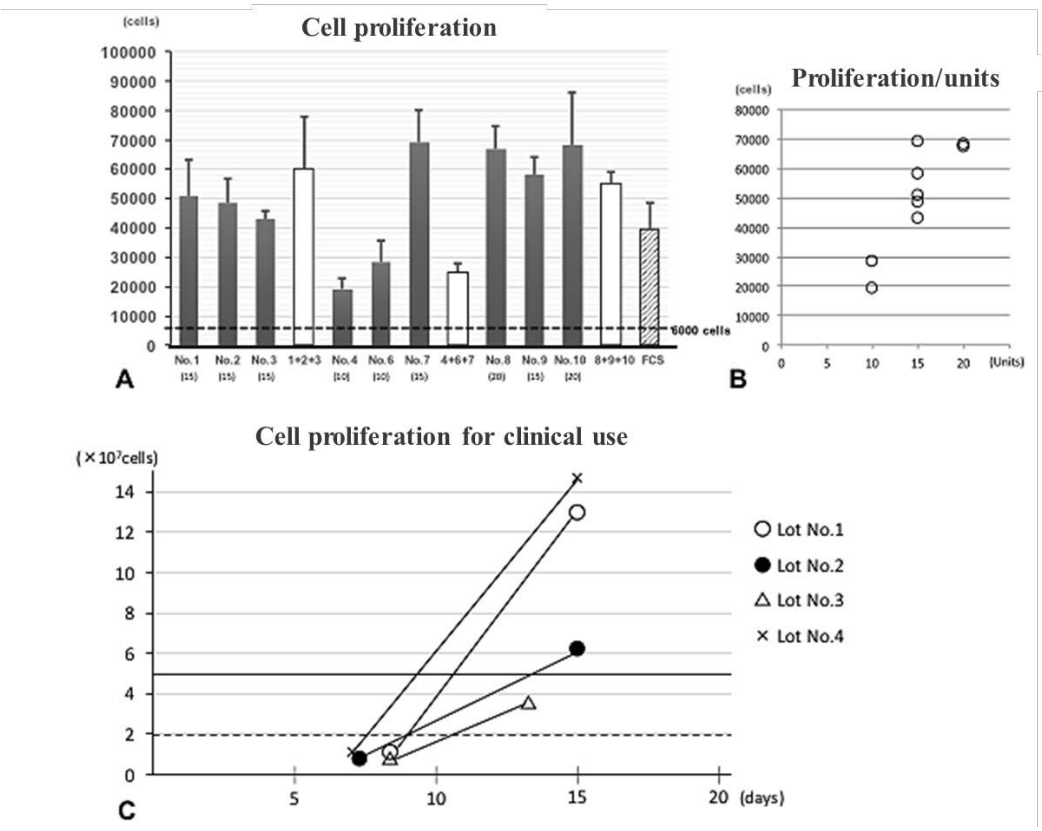

Figure 2: Cell proliferative potential for PL or FCS medium. Panel A shows the quantity of cultured cells in PL or FCS-supplemented culture medium. Gray bars: cells cultured with sPL, white bars: cells cultured with mPL, striped bar: the cells cultured with FCS. Error bars: SD. Broken line: the quantity of seeded cells on a well (6000 cells). Panel B shows the quantity of cultured cells in PL-supplemented culture medium. X-axis: numbers of the platelet units in original PC. Panel C showed the cell proliferation when cultured in CPC as a simulation of the clinical trials, the RAINBOW study. Broken line: 20 million cells as the target in the low dose group. Solid line: 50 million cells as the target in the high dose group.

Cell proliferative potential of PL

Cell proliferation assays demonstrated the expansive capacity of hBMSCs with 12 types of PL-supplemented αMEM (9 sPL and 3 mPL) or FCS-supplemented DMEM. Two weeks after cell seeding, a distinct difference existed among each quantity of cell proliferation (Fig. 2A). Compared with the cell proliferation in FCS medium, most of the PL medium had the equivalent or much higher expansive ability. However, the sPL derived from 10 unit-PC (No. 4 and No. 6) were much lower than FCS. Moreover, one of mPL, No. 4 + 6 + 7, also had a lower proliferative

potential because it was made of No. 4 and No. 6 in sPL (Fig. 2A). Thus, when the data were analyzed regarding the platelet units in original PC, we found a correlation between the unit number and proliferative potential (Fig. 2B). Moreover, the proliferative potential was positively correlated with the concentrations of PDGF-BB (r = 0.74), TGF-β1 (r = 0.80), and BDNF (r = 0.73, Fig. 3B)

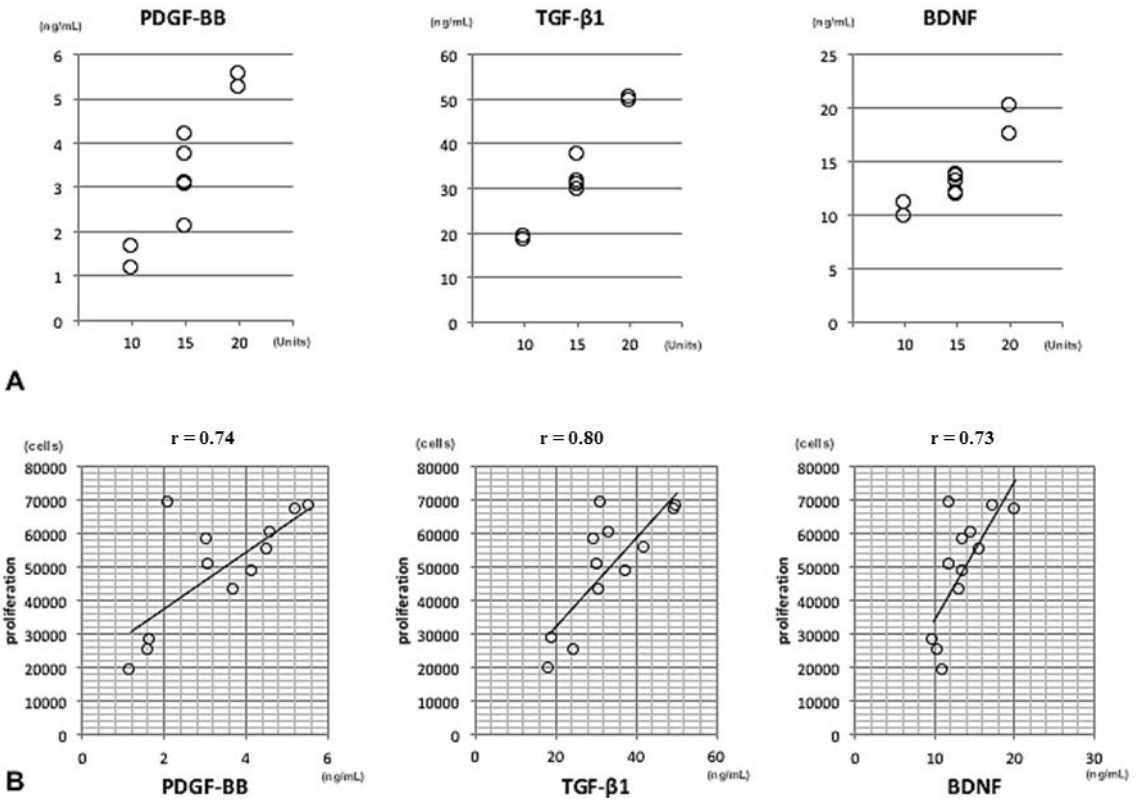

Figure 3: Cell proliferative potential and growth factors. Panel A shows the concentration of each growth factor (left: PDGF-BB, center: TGF-β1, right: BDNF). X-axis: numbers of the platelet units in original PC. Panel B shows the correlation between cell proliferative potential and the concentration of each growth factor (left: PDGF-BB, center: TGF-β1, right: BDNF).

The hBMSCs derived from 4 healthy volunteers (Lot. No. 1, 2, 3, and 4) were cultured in CPC as a simulation of the RAINBOW study (phase 1 clinical trial, the Research on Advanced Intervention using Novel Bone Marrow Stem Cell; Fig. 2C). The cells in each lot were passed first on the day 7 or 8 after the culture. The cells in 3 lots were passed second on the day 15, and the cell numbers in each lot reached over 5×10^7 cells which is the target in the high dose group. On the other hand, the cells in Lot No. 3 were passed second on day 13 and the cell numbers reached 3.5×10^7 cells. In Lot No. 3, the numbers of hBMSCs were over 20 million

which is the target in the low dose group, but not the high dose one (Fig. 2C).

Surface marker of hBMSC

Flow cytometric analysis was performed to assay the surface markers of hBMSCs cultured with PL-supplemented αMEM. These cells expressed CD44 (96.5 ± 2.5 %), CD90 (97.3 ± 3.5 %), CD105 (98.5 ± 0.6 %), CD106 (51.5 ± 14.8 %), CD146 (36.8 ± 18.1 %), and CD166 (97.8 ± 1.5 %), while there was an absence of CD19 (2.8 ± 1.7 %) and CD45 (1.8 ± 0.5 %) (n=4 in each, Fig. 4).

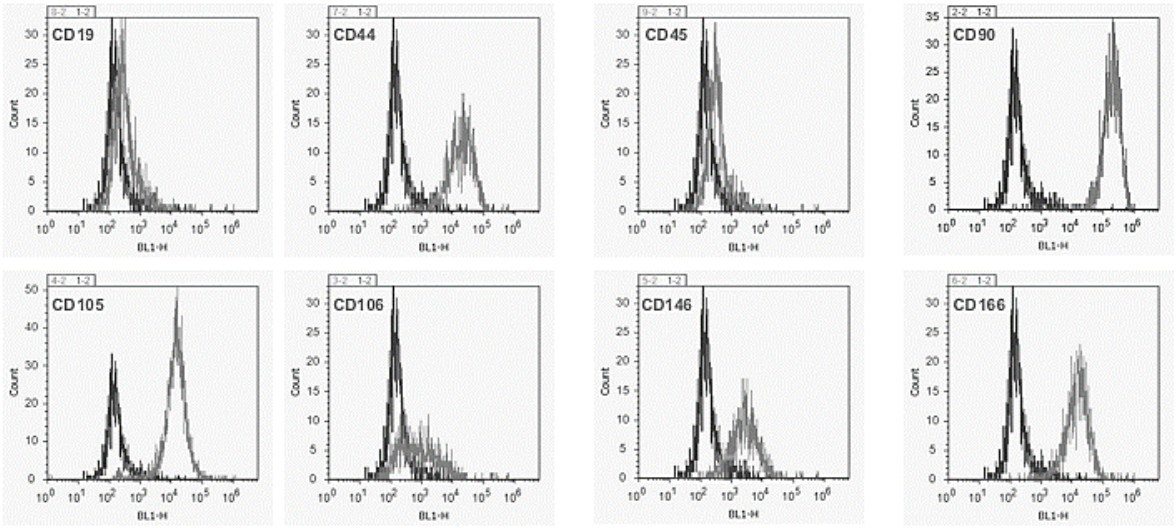

Figure 4: Flow cytometric analysis of the surface markers. Gray lines: each specific antibody (CD44, CD90, CD105, CD106, CD146, CD166, CD19, and CD45), black lines: each isotopic antibody.

SPIO-labeled hBMSC and QSM MRI

Turnbull's Blue staining demonstrated that approximately 34% of the PL-cultured hBMSCs were labeled with SPIO 24h after incubation with SPIO nanoparticles (Fig. 5A). The MRI for clinical use could visualize the bolus of SPIO-hBMSCs engrafted in the decapitated pig brain. The cell bolus showed a strong signal loss when imaged with QSM methods (Fig. 5B). Histological analysis clearly revealed that some SPIO-positive cells (Fig. 5C) or human cells (Fig. 5D) were found around the injection region. These findings were consistent with the results of MRI.

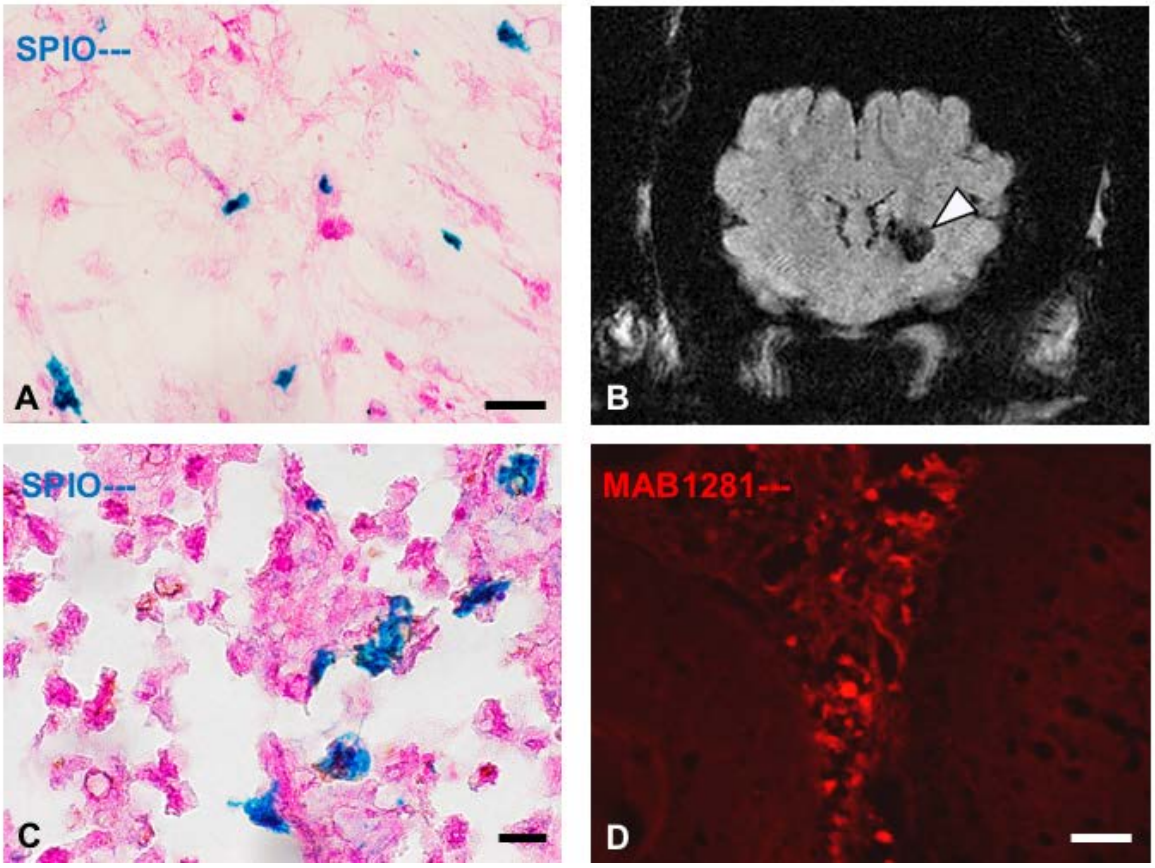

Figure 5: MRI and histological analysis of pig's brain with SPIO-labeled hBMSC injection. Panel A shows the photomicrographs of the cultured SPIO-hBMSCs after Turnbull's Blue staining (blue: SPIO). Scale bars: 50μm. Panel B represents QSM MR images. Arrowheads indicate the signal extinctions caused by the bolus of SPIO-labeled hBMSCs in the left striatum. Panels C and D display representative photomicrographs of the region around the SPIO-hBMSC injection after Turnbull's Blue staining (blue: SPIO, Panel C) and fluorescence immunostaining (red: MAB1281, Panel D). Scale bars: 20 μm (Panel C), 50 μm (Panel D).

DISCUSSION

In the present study, we harvested 12 kinds of human PLs as growth supplements instead of FCS. ELISA analysis showed that PL contained adequate growth factors and very small amount of platelet surface antigens. Although the PL had equivalent or higher cell proliferation capacity compared with FCS, there was no contradiction to BMSC for cell surface markers in hBMSC-PL. About 2 weeks, the cell numbers could reach up to 2×10^7 cells which is the target in our clinical trials in every lots. When SPIO-labeled hBMSCs were injected into the pig brain, MRI could detect their distribution the same as histological analysis.

When PL products are made from human PRP in accordance with good manufacturing practice (GMP), we noticed the existence of fragments of platelet membranes as residue

materials which are a source for inducing immune response. Instead of fragments of platelet membranes, we analyzed the platelet surface antigens in PL products because it is difficult to detect the residual fragments themselves. In the present study, we detected a very small amount of CD61, but not CD41. The findings suggested that the amount of CD61 in PL was useful for quality control of residue materials when produced on GMP level. In fact, the mean content of CD61 in PL was 210 ± 63 pg/mL (the lower limitation of detect range: 125 pg/mL) in our present data., so the presence of CD61 is unable to be detected in culture medium because only 10% PL was added to the medium and filtering was employed to reduce the impurity. This finding demonstrated that our PL products held adequate safety and quality for clinical application.

Various studies have indicated that growth factors such as PDGF-BB, TGF-β1, and BDNF play a prominent role in BMSC culture. PDGF-BB can elicit a mitogenic response from BMSCs and stimulates these cells to proliferate[55-57]. It has also been demonstrated that TGF-β1 could stimulate the proliferation of undifferentiated MSC[55,58]. In contrast, our previous report showed that the concentration of human BDNF, which was derived from PL, markedly decreased in the medium after hBMSC culture. These results strongly suggested that the cultured hBMSCs may consume human BDNF for their survival and proliferation[38] . In the present study, we found that the content of these growth factors in each PL was relevant to the amount of platelets in original PC. Furthermore, the ability of cell expansion correlated with the contents of the growth factors in each PL. When the contents of platelets in original PC reached more than 15 units, the cell proliferating potential of PL was equivalent or much higher compared with the FCS. This indicated that the PL-supplement contains adequate essential growth factors and nutrition as well as FCS for the expansion of hBMSC. When made in accordance with GMP, however, the findings suggested that we could check the contents of a growth factor, PDGF-BB, TGF-β1, or BDNF as a quality control of PL products instead of the potential for cell expansion. Moreover, because there was a smaller difference among mPL compared with sPL regarding the contents of growth factors, pooled PL should be useful in mass production.

It is well known that hBMSCs express CD44, CD90, CD105, CD106, CD146, and CD166 but not CD14, CD19, CD34, and CD45[59-61]. In our previous study, no significant differences

were observed between hBMSCs cultured using 5% PL and using 10% FCS[38]. In the present study, although the concentration of PL was changed to 10%, we confirmed that the hBMSCs were identical for surface markers. Thus, our findings demonstrate that 10% PL-cultured hBMSCs are reliable for clinical application as well as 5% PL-cultured cells. In the productions of hBMSC products, moreover, the present results suggested that CD44, CD90, CD105, and CD166, but not CD106 or CD146, should be suitable positive makers for the specific test, because of their high percentage and low SD.

In our new clinical trials, RAINBOW study, the subjects are acute ischemic stroke patients. Autologous bone mallow is obtained 2 weeks after the stroke onset. And then BMSCs are cultured with allogeneic PL in CPC up to 2 cell doses; 20 million cells in the low dose group and 50 million cells in the high dose one. In the present study, the cell numbers could reach up to 5×10^7 cells in only 3 lots, though the numbers could increase over 2×10^7 cells in every 4 lots 2 weeks after the start of culture. So we decided to translate the results to the protocol of RAINBOW study. Thus, in the patient allocated to the high dose group, the patient would be shifted to the low dose group if the cell numbers could not reach up to 5×10^7 cells in a period.

In addition, hBMSCs were visualized in a decapitated pig brain. Cell labeling with SPIO was employed to track donor cells in the host brain by means of MRI. Cultured hBMSCs can uptake SPIO nanoparticles into their cytoplasm when the particles are added to the culture medium[62]. In the present study, Turnbull's Blue staining analysis showed that 34% hBMSCs in a chamber slide contained SPIO nanoparticles. Because SPIO nanoparticles have clearly detectable signal extinctions, SPIO-labelled cells were easily tracked anatomically with QSM MR images [62]. Histological analysis gained the same hBMSC distribution compared with MRI. Our previous study identified the long term safety of SPIO-labeled BMSCs[62]. Thus, we believe that MRI cell tracking with SPIO based labeling agents is a good resource to monitor cell distribution after hBMSC transplantation. We hope this technology can be used for cell therapy in clinical applications.

Chapter II

Short-, middle- and long-term safety of superparamagnetic iron oxide-labeled allogeneic bone marrow stromal cell transplantation in rat model of lacunar infarction

INTRODUCTION

BMSCs have been regarded as potential cells in regenerative medicine. In addition, allogeneic cell sources as off-the-shelf products have advantaged, such as lower invasiveness, fewer limitations on the timing of administration, and a lower cost of treatment. However, the fate of allogeneic BMSCs and the resulting immunological reaction after the transplantation for the treatment of stroke are still unknown. To gain a better understanding of the cellular fate in various biological processes, a range of imaging techniques have been proposed to render transplanted cells visible.

The SPIO is composed of nano-sized iron oxide crystals coated with dextran or carboxydextran and available as clinical MRI contrast agents for liver. Although SPIO was not originally designed for cell tracking, due to its high labeling rates, long half-life, and high resolution on MR imaging, it has been optimized for the imaging of stem cells in clinical investigations on the basis of numerous animal studies[63-67]. Ferucarbotran (Resovist®), one of the representative SPIO agents, is composed of a 60 nm particle coated with carboxydextran, and it is accumulated by phagocytosis in a cell body[68,69]. Uptake of SPIO in the cells decreases the signal intensity on MRI. When the SPIO-labeled cells are transplanted in the brain, their position can be tracked by monitoring on T2-weighted images[68]. However, at present, the detailed safety evaluation of SPIO-labeled BMSCs still remains undetermined. Therefore, this study aimed to investigate and evaluate the short-, middle- and long-term safety of the SPIO-labeled BMSCs in rat lacunar infarction model.

MATERIALS AND METHODS

Isolation and culture of BMSCs from rats

All animal experiments were approved by the Animal Studies Ethical Committee at Hokkaido University Graduate School of Medicine. The BMSCs were isolated from 7-week-old green fluorescence protein (GFP)-transgenic rats (Japan SLC, Inc., Hamamatsu, Japan). Anesthesia was induced with 4% isoflurane in N_2O/O_2 (70:30) and maintained via spontaneous ventilation with 2% isoflurane in N_2O/O_2 (70:30). The femora were aseptically dissected. Both ends were cut and the marrow was rinsed with 5ml DMEM containing 10% FCS, 1% P/S, and 10% heparin, using a 2.5ml syringe and a 21-gauge needle.

The cell suspension was collected and centrifuged at 800 xg for 5 minutes at 15°C. The pellet was suspended in DMEM culture medium (Sigma-Aldrich, St. Louis, MO). Cells were seeded in a 150cm^2 collagen-coated flask with 25ml DMEM containing 10% FCS and 1% P/S. Then these cells were cultured in an incubator with 5% CO_2 at 37°C. After 48 hours, the non-adherent cells were removed by changing the medium. The culture medium was replaced 2 or 3 times a week. GFP-BMSCs were passed three times for subsequent transplantation.

At 24 h before transplantation, 1μl/ml Ferucarbotran (27.9μg Fe/ml, Resovist®, Fujifilm RI Pharma Co., Ltd., Tokyo, Japan) was added into the culture medium to be incubated with BMSCs. The labeled BMSCs in flask were lifted by 4ml 0.25% trypsin and 0.02% EDTA in PBS and put into the incubator for 5 min. After agitating fully, the BMSCs liquid was transfer into a test tube and centrifuged by 800 xg, 5min at 15°C. The supernatant was decanted and the cells were gently resuspended by PBS.

Rat lacunar infarct model

Wistar rats (male, 240-260g) were used to make lacunar infarction models. Ouabain (a Na/K ATPase pump inhibitor, Sigma, St. Louis, MO) or vehicle was stereotactically injected into the right striatum to induced lacunar lesion. Anesthesia was as same as above mention. The animals were fixed to a stereotactic apparatus (Model DKI-900, David Kopf Instruments, Tujunga, CA). A burr hole was made 3mm right to the bregma, using a small dental drill. A Hamilton syringe

was inserted 5mm into the brain from the surface of dura mater, and 1μl of 2.5mM ouabain was injected over 5min, using an automatic microinjection pump (Model KDS-310, Muromachi Kikai Co., LTD.,Tokyo, Japan). After injection, the needle was left *in situ* for 5min to avoid leakage of the injected fluid through the needle tract[54,3].

BMSC transplantation

Seven days after the insult, BMSC suspension (or SPIO solution) were stereotactically transplanted into the left striatum. Briefly, a burr hole was made 3mm left to the bregma. A Hamilton syringe was inserted 4mm into the brain parenchyma. Then, 10μl (5×10^5cells) of BMSC suspension was injected into the left striatum over 5min, using an automatic microinjection pump. All animals in the whole groups were subcutaneously injected immunosuppressive drug Cyclosporine A (CsA, 10mg/kg; Novartis Pharma K.K., Tokyo, Japan) daily up to 6 weeks after transplantation.

Serial MR tracking of transplanted BMSCs in vivo

The behaviors of transplanted BMSCs were serially monitored from 1 to 42 days after BMSC injection by an MRI apparatus (n=4). All MR imaging was acquired using a small animal, horizontal bore, 7.0-Tesla MR scanner (Unity INOVA, Varian, Inc., Palo Alto, CA) interfaced to a VNMR console (Varian Inc.). In order to administrating anesthetic gas and minimizing error in the repeatability of head positioning, the rat was anesthetized with a nose cone and placed on nonmagnetic holder. Using feedback-controlled water bath, the core temperature was kept between 36.5°C and 37.5°C, during the imaging procedure. Coronal T2-weighted images are obtained by standard two-dimensional Fourier transform, multislice (nine slices, 1 mm thick) and spin echo T2 sequence to detect the SPIO-labeled BMSCs in the brain. The T2 sequence parameters were as follow: TR = 2 500ms, TE = 60ms, AC = 4 times, field of view (FOV) = 30 × 30mm, and matrix = 512 × 512[70,3].

Histological analysis

All animals were used for histological analysis after their sacrifice (n=22). Sixteen rats were treated with ouabain and BMSCs, and they were sacrificed 7 days after transplantation (7 days group; n=7), 6 weeks (6 weeks group; n=6), or 10 months (10 months A group; n=3), respectively. The other animals, which were treated with ouabain and SPIO solution (10 months B group; n=1), with vehicle and BMSCs (10 months C group; n=2), and with vehicle and SPIO solution (10 months D group; n=3), were sacrificed 10 months after transplantation.

Animals were deeply anesthetized and transcardially perfused with 20ml of heparinized saline, followed by 50ml of 4% paraformaldehyde. The brains were removed and protected into the 4% paraformaldehyde with low temperatures. They were sliced and embedded in paraffin. Paraffin sections of a 4 μm thickness were mounted onto silane-coated glass slides. The sections were stained with Hematoxylin and Eosin (HE) and Turnbull Blue method to evaluate the distribution of SPIO-labeled BMSCs.

In multi-staining immunohistochemistry, for antigen retrieval, deparaffinized sections on glass slides were immersed into 0.01mol/l pH6.0 citric acid buffer solution (LSI Medience, Tokyo, Japan) and heating treated by pressure pot for 2min. These sections were pretreated with peroxidase blocking reagent (Dako Japan, Tokyo, Japan), and then incubated by 1% block ace solution (DS Pharma Biomedical, Osaka, Japan) for 30min. The sections were treated with rabbit polyclonal antibody against Iba1 (1:2000 dilution, Wako, Osaka, Japan) at 37℃ for 1h. After Simple Stain AP (M) (Nichirei, Tokyo, Japan) was used, New Fuchsin substrate kit (Nichirei, Tokyo, Japan) was applied to color GFP-BMSCs. Then, the sections were heating treated again to deactivate the first antibody for the following stain with primary antibody against GFP (rabbit monoclonal, 1:200 dilution, Cell Signaling, Danvers, MA) at 37℃ for 1h. DAKO EnVision+Kit and DAB Substitute Kit (Dako Japan, Tokyo, Japan) were employed according to their instructions. After the staining, these sections were dipped into 10% ammonium sulfide solution (Sigma-Aldrich, St. Louis, MO) overnight, followed by incubation with compound solution mixed by 20% potassium ferricyanide (Wako, Osaka, Japan) and 1% HCl solution 20min. Hematoxylin was used for counterstaining. A few sections were treated with antibody against Iba1 (1:2000 dilution, Wako, Osaka, Japan) merely, and then were colored

with DAKO EnVision+ kit and DAB substitute kit (Dako Japan, Tokyo, Japan).

For fluorescent immunohistochemistry, after the sections were processed for antigen retrieval and blocking of non-specific reaction, rabbit polyclonal anti-Iba1 antibody (1:1500 dilution, Wako, Osaka, Japan) and mouse monoclonal anti-CD68 antibody [ED1] (1:80 dilution, abcam, Cambridge, England) were applied at 37℃ for 1h. As secondary antibodies, they were incubated with Alexa Fluor 594 Goat Anti-Rabbit IgG (H+L) Antibody and Alexa Fluor 350 Goat Anti-Mouse $IgG_1(\gamma 1)$ (1:200 dilution, Life Technologies, Carlsbad, CA) at 37℃ for 1h, respectively. Subsequently, they were incubated with the rabbit monoclonal antibody against GFP (1:80 dilution, Cell Signaling, Danvers, MA) tagged with a fluorescence label, Zenon Alexa Fluor 488 Rabbit IgG Labeling Kit (Life Technologies, Carlsbad, CA), at room temperature for 1h. A few sections were treated with antibody against GFP (1:80 dilution, Cell Signaling, Danvers, MA) or antibody against neuronal nuclear antigen (NeuN; 1:400 dilution, Chemicon, Temecula CA) merely, and then were colored with Alexa Fluor 488 Goat Anti-rabbit IgG Antibody (1:200 dilution, Life Technologies, Carlsbad, CA) or Alexa Fluor 594 Goat Anti-mouse IgG Antibody (1:200 dilution, Life Technologies, Carlsbad, CA). Some of sections were counterstained with DAPI (Invitrogen). The fluorescence emitted was observed on fluorescence microscope (BX51, Olympus, Tokyo, Japan) and was digitally photographed using a cooled CCD camera (model VB-6000/6010, Keyence, Osaka, Japan).

RESULT

SPIO-labeled BMSCs

Turnbull blue staining demonstrated that most of the cultured BMSCs were labeled with SPIO 24 h after the incubation with SPIO nanoparticles (Fig. 6A). However, it was found that the amount of SPIO nanoparticles in the cell body was decreasing with time. When 7 days passed, because of the cell division, the nanoparticles were diluted within each cell (Fig. 6B–D). In contrast, it was found that all cultured cells could express green fluorescence derived from GFP (Fig. 6D).

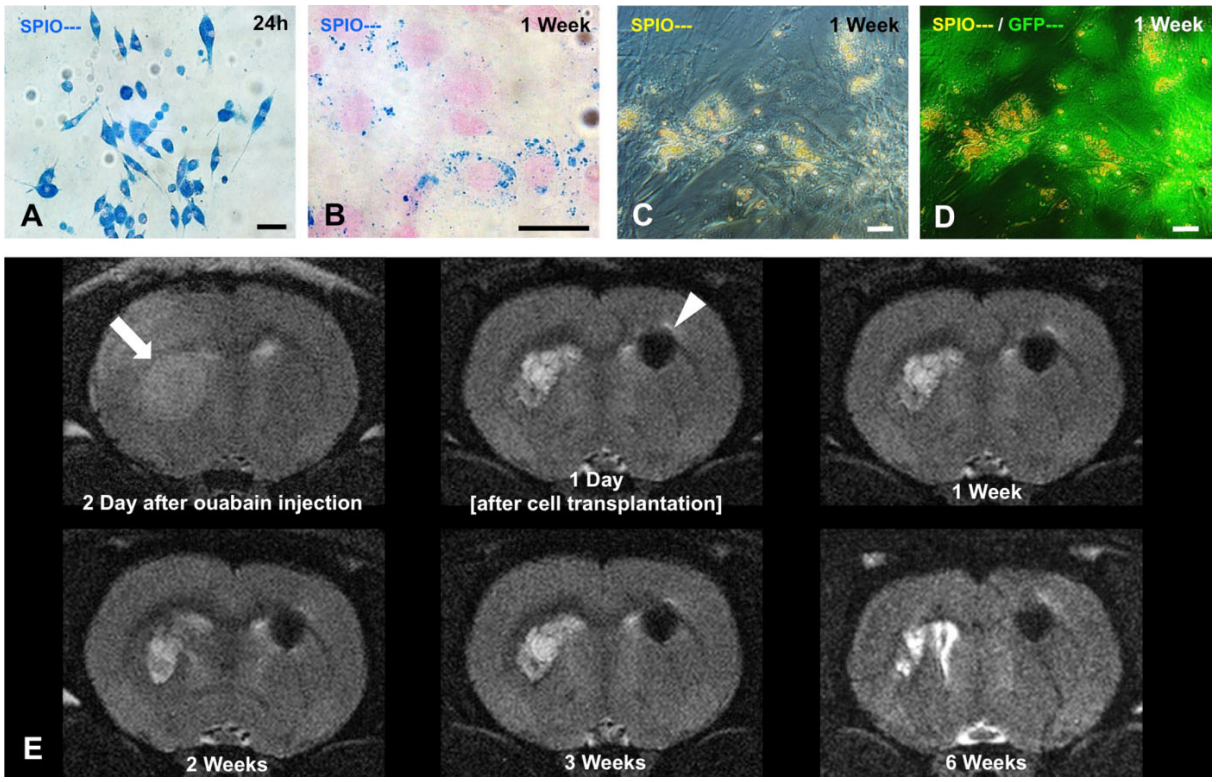

Figure 6: The cultured SPIO-BMSCs and MRI. Panels A–D show representative photomicrographs of cultured GFP-BMSCs (A: 24 h after the incubation with SPIO, B–D: 7 days after the incubation). Panels A and B show Turnbull blue staining (blue: SPIO). Panel C shows the image obtained using a polarizing microscope and panel D is a merged picture with a fluorescent image (yellow: SPIO, green: GFP). Scale bars: 100 μm (A), 50 μm (B), and 20 μm (C, D). Panel E shows serial T2-weighted MRI images. Arrows show the ouabain-induced lesion in the right striatum. Arrowheads indicate the signal extinctions caused by the bolus of SPIO-labeled BMSCs in the left striatum.

Serial T2-weighted MRI

MRI could serially monitor the ouabain-induced lesion. In addition, it could track SPIO-BMSCs in the brain, leading to a decreased signal in their accumulation when imaged with T2-weighted images (Fig. 6E). Two days after the ouabain injection, MRI clearly showed the lesion in the right striatum with a high intensity area, which was determined to be not only an ischemic but also an extensive edematous lesion. One day after the cell transplantation, the bolus of SPIO-labeled BMSCs revealed a strong signal loss in the left striatum. Until 3 weeks after the transplantation, MRI showed low signal intensity in the corpus callosum and right external capsule. This result suggested that SPIO-labeled BMSCs may start to migrate through the corpus callosum to the lacunar lesion. Six weeks after the transplantation, MRI showed a smaller lesion area and a ventricular dilatation. Because low signal intensity was seen around

the lacunar lesion, SPIO-labeled BMSCs may have reached the lesion through the corpus callosum (Fig. 6E).

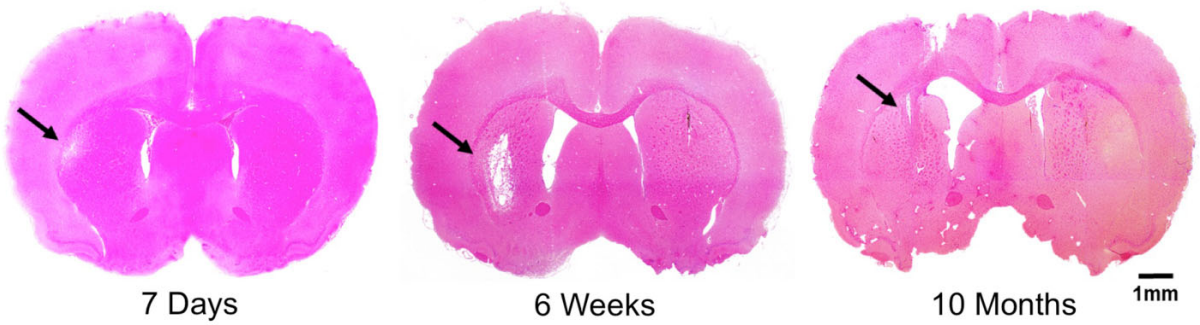

Figure 7: HE staining. Arrows indicate the ouabain-induced lesion in the right striatum. Scale bar: 1 mm.

Histological analysis of the 7-day group

HE staining showed that the ouabain-induced lacunar lesion was located in the right striatum 7 days after the transplantation (Fig. 7). Turnbull blue staining revealed that some SPIO-positive cells were found not only in the transplantation area but also in the corpus callosum, in distal white matter on the transplantation side, and around the lacunar lesion (Fig. 8). These findings were consistent with the results of MRI.

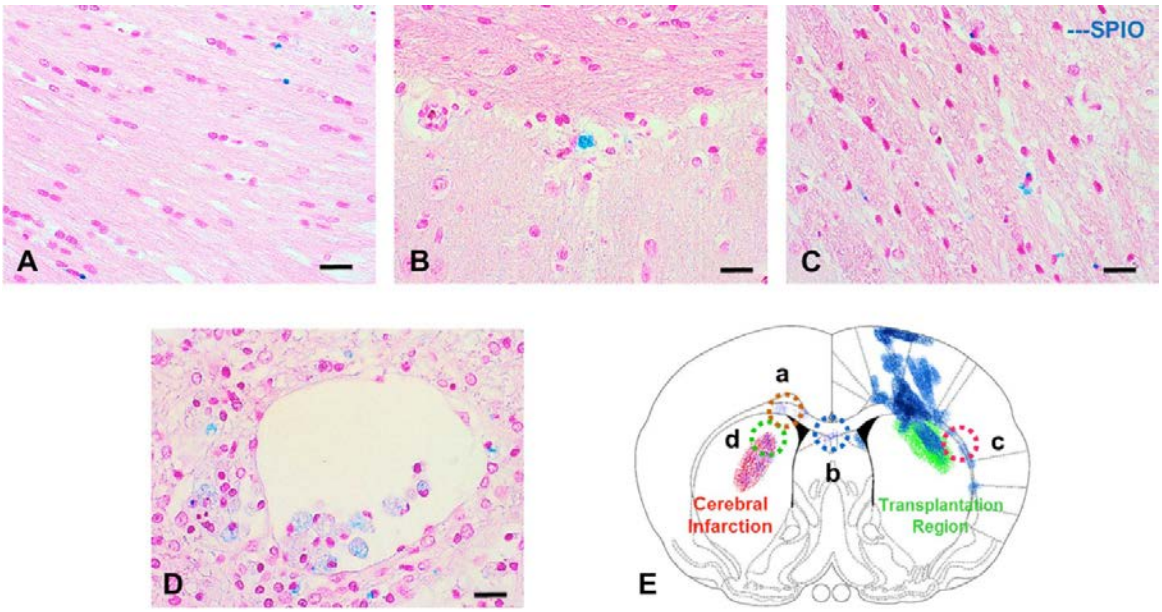

Figure 8: Turnbull blue staining in the 7-day group. Panels A–D show photomicrographs in the 7-day group (A and B: corpus callosum, C: white matter in the transplanted side, D: the lacunar infarction area; blue: SPIO. Scale bars: 20 μm. Panel E is a schematic diagram that shows the location of the lacunar infarct (red), distribution of the SPIO-positive cells (blue) and the location of panels A–D (broken circles) in the brain of rats from the 7-day group.

In the 7-day group, immunohistochemistry with Turnbull blue staining showed that microglia migrated and concentrated around the lacunar infarction and cell transplantation area (Fig. 9A–C). Interestingly, there were many GFP-positive cells without SPIO in the donor cell bolus (Fig. 9B). It was suggested that SPIO-labeled GFP-BMSCs may have survived and began to proliferate there.

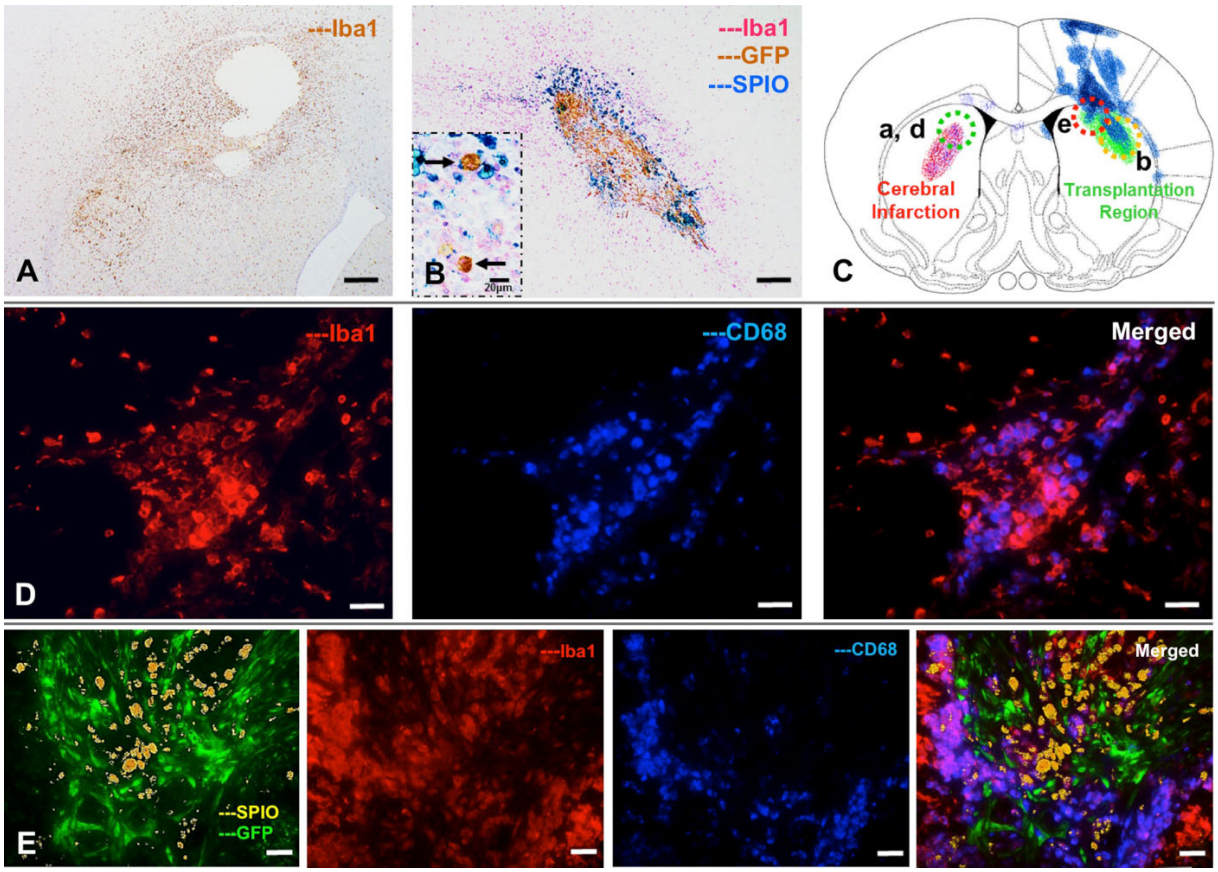

Figure 9: Immunohistochemical analysis in the 7-day group. Panels A and B show representative photomicrographs with immunohistochemistry and/or Turnbull blue staining. Panel A shows the area around the lacunar infarction (brown: Iba1), and panel B shows the area around the transplantation site (pink: Iba1, brown: GFP, blue: SPIO. Scale bars: 500 μm (A) and 200 μm (B). Panel D shows the area around the lacunar infarction (red: Iba1, blue: CD68), and panel E shows the area around the transplantation site (red: Iba1, blue: CD68, green: GFP, yellow: SPIO). Scale bars: 20 μm. Panel C is a schematic diagram that indicates the location of the lacunar infarct (red), distribution of the SPIO-positive cells (blue), and the location of panels A, B, D and E (broken circles) in the brain of rats from the 7-day group.

Fluorescent immunohistochemistry clearly revealed the relationship among the lacunar lesion, BMSCs and microglia in the host brain. Immunoreaction for CD68, a marker for microglial activation, demonstrated that a large number of activated microglia aggregated and surrounded the lacunar infarction area (Fig. 9D). By means of cell counting, 80.7% of microglia

expressed M1 phenotype ($CD68^+$) in the infarction area. In the transplantation area, it was also found that many activated microglia aggregated and surrounded the bolus of donor cells (Fig. 9E). Double immunostaining against GFP and NeuN showed that BMSCs had no tendency toward neural differentiation in the transplantation area and around the lacunar lesion (Fig. 12A).

Histological analysis of the 6-week group

Compared with the 7-day group, the animals of the 6-week group had a ventricular dilatation in the hemisphere on the infarction side (Fig. 7). Following migration of donor cells, a few SPIO-positive cells and more GFP-positive cells were found in the corpus callosum (Fig. 10). On the other hand, more SPIO-positive cells and GFP-positive cells were found in the area adjacent to the lacunar infarct compared with the 7-day group (Fig. 11A, B, and F). These findings about SPIO-positive cells accord with the MRI result (Fig 11E). A part of SPIO-positive cells co-expressed Iba1 (Fig. 11C). It suggested that some microglia may phagocytize some SPIO particles released from dead donor cells, but there was no evidence of BMSCs' differentiation into microglia. No double-positive cells with GFP and Iba1 were observed (data not shown). In contrast, there were fewer SPIO-positive cells in the transplanted area compared with the 7-day group. Although some M1 phenotype microglia were also found around the transplantation area, the number of activated cells was much lower compared with the 7-day group (Fig. 11D). The same phenomenon was found in the infarction side (Fig. 11E), and only 18.3% microglia expressed M1 phenotype in the infarction area. On the other hand, some BMSCs had a tendency toward neural differentiation around the infarction lesion (Fig. 12B).

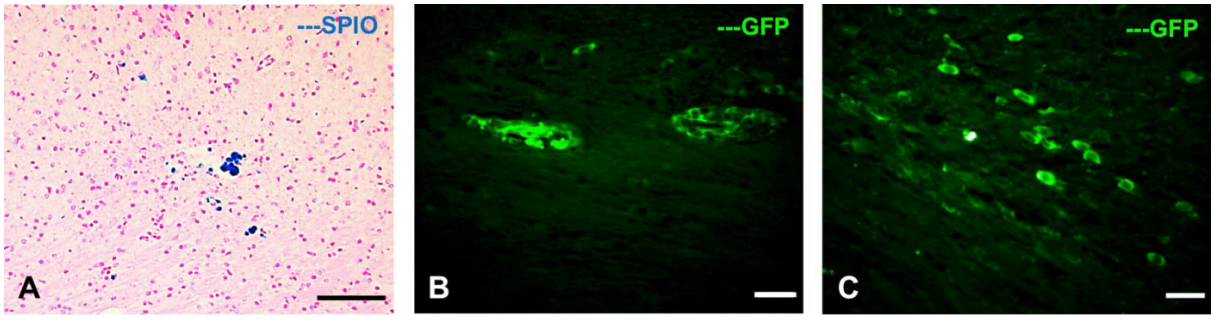

Figure 10: The BMSCs in corpus callosum of the 6-week group. Turnbull blue staining (A) and fluorescent immunostaining (B and C, green: GFP) show the existence of BMSCs in corpus callosum of the 6-week group. Scale bars: 50 μm (A), 20 μm (B, C).

Interestingly, we also found that some SPIO-positive cells and a few GFP-positive cells got attached to blood vessels on both the transplantation and infarction sides (Fig. 13A, D). Although most SPIO nanoparticles were engulfed by microglia (Fig. 13B), others were not (Fig. 13C). These results were also observed in both the 7-day group and 10-month group A.

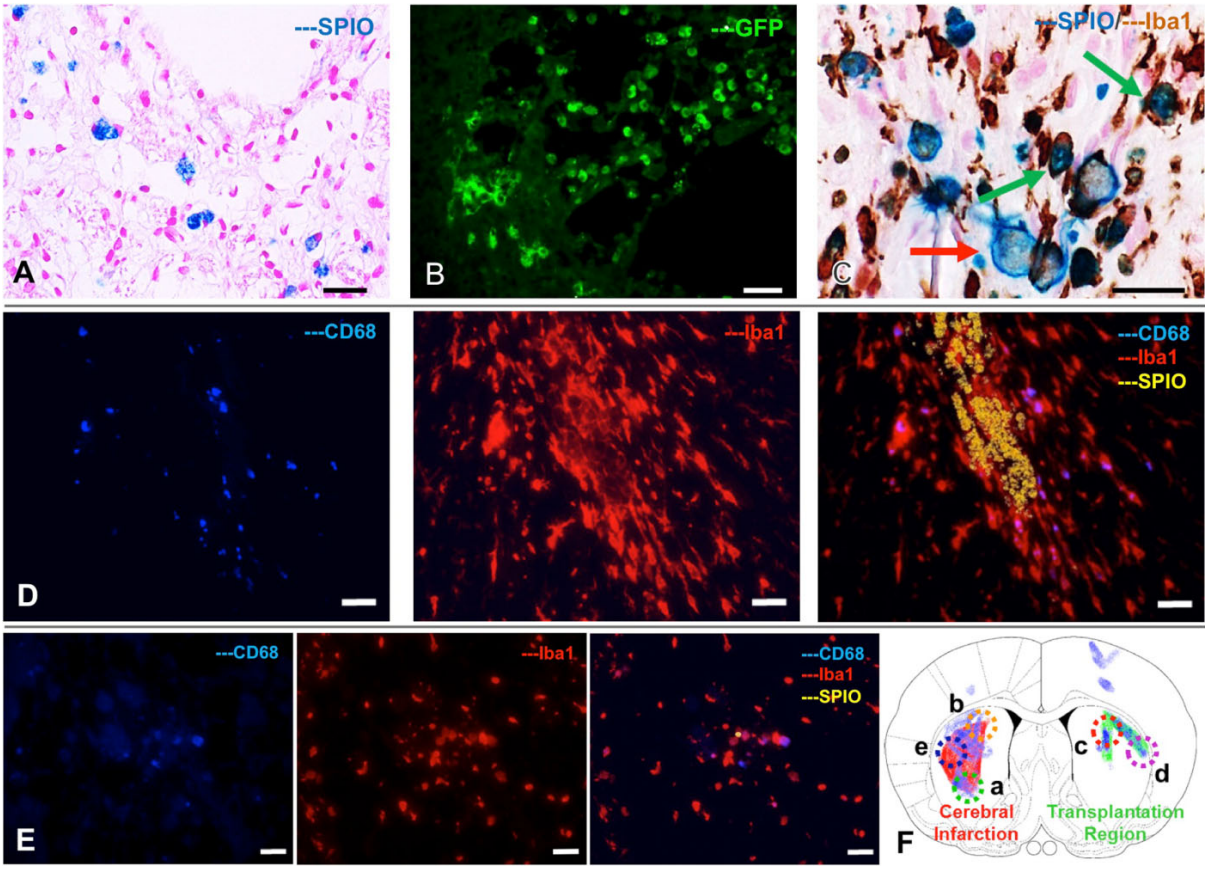

Figure 11: Turnbull blue staining and immunohistochemical analysis in the 6-week group. Panels A and B show representative photomicrographs around the infarct lesion (A, blue: SPIO; B, green: GFP). Scale bars: 20 μm. Panels C and D show representative photomicrographs around the transplantation site (C, brown: Iba1, blue: SPIO; D, blue: CD68, red: Iba1, yellow: SPIO). Panel E shows the infarction area (blue: CD68, red: Iba1, yellow: SPIO). Scale bars: 20 μm. Panel F is a schematic diagram that indicates the location of the lacunar infarct (red), distribution of the SPIO-positive cells (blue) and the location of panels A–D (broken circles) in the brain of rats from the 6-week group.

Histological analysis of the 10-month groups

In the 10-month group A, HE showed a scar formation in the lacunar lesion and ventricular dilatation on the ipsilateral side (Fig. 7). The SPIO-positive cells were extensively spread in both hemispheres, but the number of cells was lower than in the 6-week group. Some SPIO-positive cells were seen along the route of the cell transplantation (Fig. 14A) and the lacunar area (Fig. 14B). None of the animals were observed to develop either a tumor or severe inflammation.

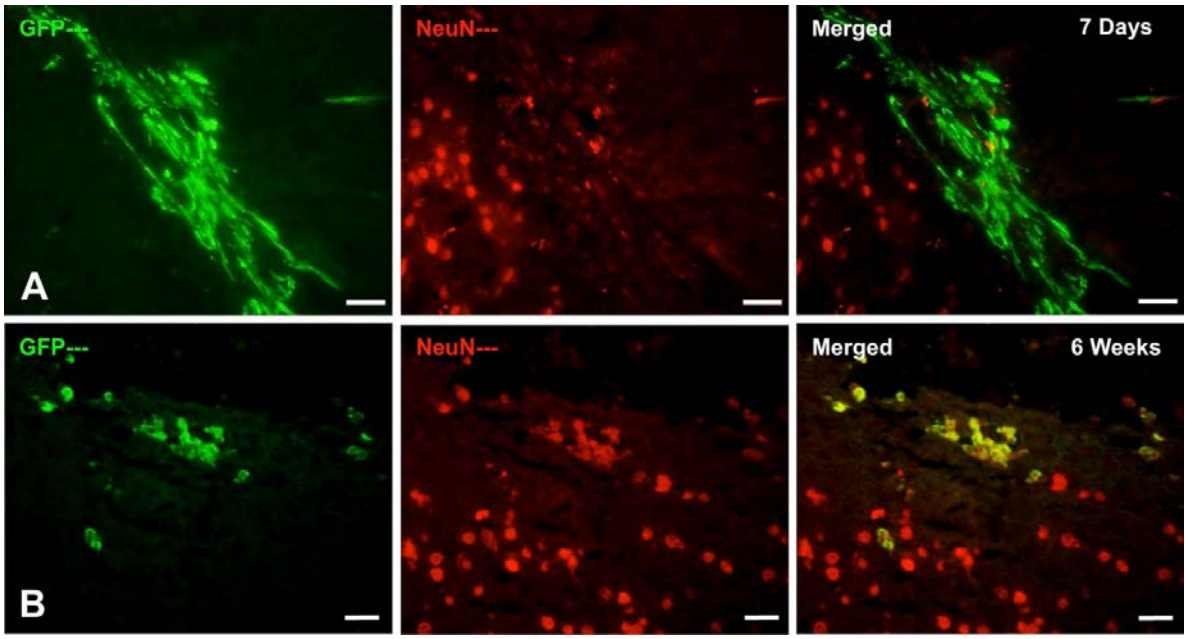

Figure 12: Immunofluorescence exhibits the situation of neural differentiation of BMSCs. Panel A represents the transplantation area of the 7-day group. Panel B shows infarct lesion of the 6-week group (green: GFP, red: NeuN). Scale bars: 20 μm.

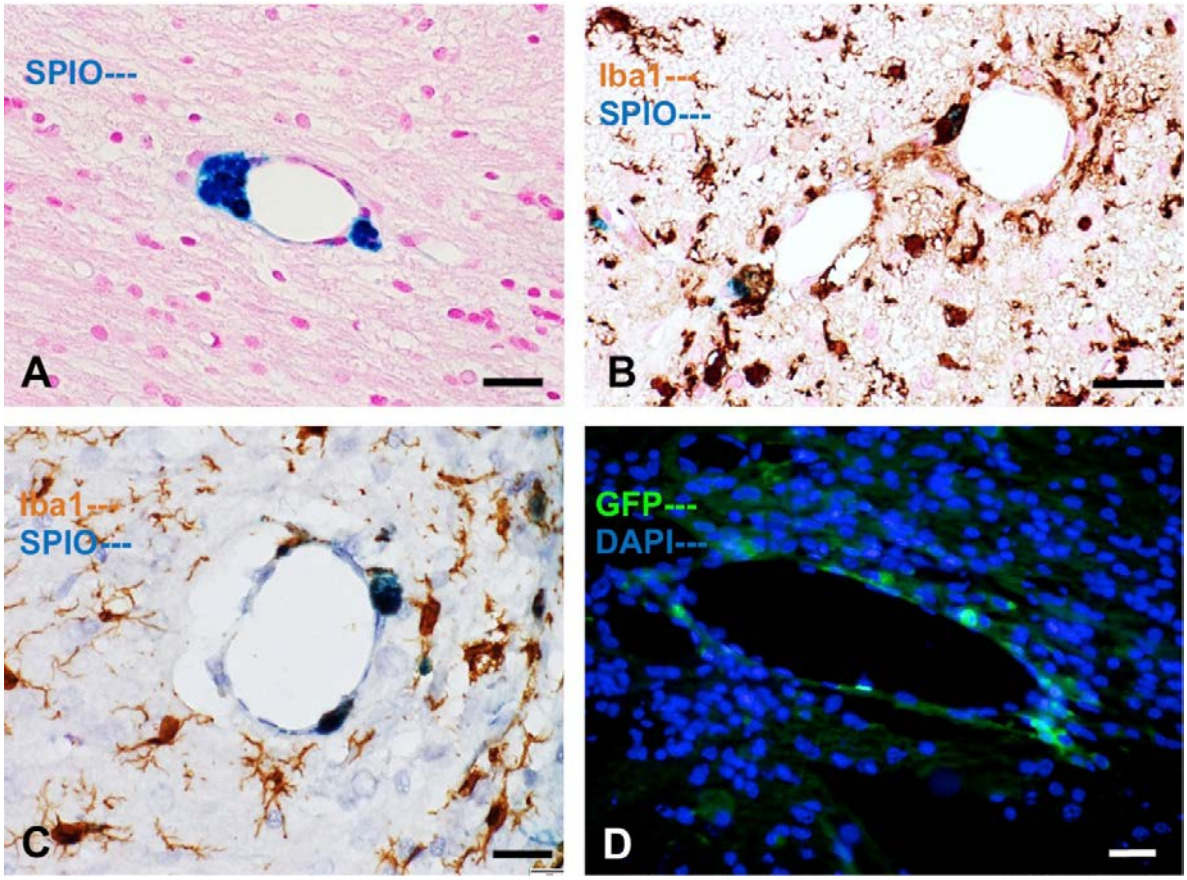

Figure 13: The relationship between SPIO-positive cells and blood vessels. Panel A shows a representative photomicrograph with Turnbull blue staining (blue: SPIO). Panels B and C show representative photomicrographs with immunohistochemical analysis and Turnbull blue staining (brown: Iba1, blue: SPIO). Panel D shows representative photomicrographs with fluorescent immunostaining (green: GFP, blue: DAPI). Scale bars: 20 μm.

In the 10-month group B, animals had lacunar infarction and injection of the SPIO solution in the opposite side. Although a few of the SPIO nanoparticles were found along the injection track (Fig. 14D), immunohistochemical staining for Iba1 showed absence of severe tissue inflammation (Fig. 14E).

In both the 10-month C and D groups, because there was no ouabain-induced lesion in the brain, SPIO-positive cells or SPIO nanoparticles were unable to migrate anywhere; therefore, they stayed along the injection track. No animals had signs of severe brain injury around the injection area (data not shown).

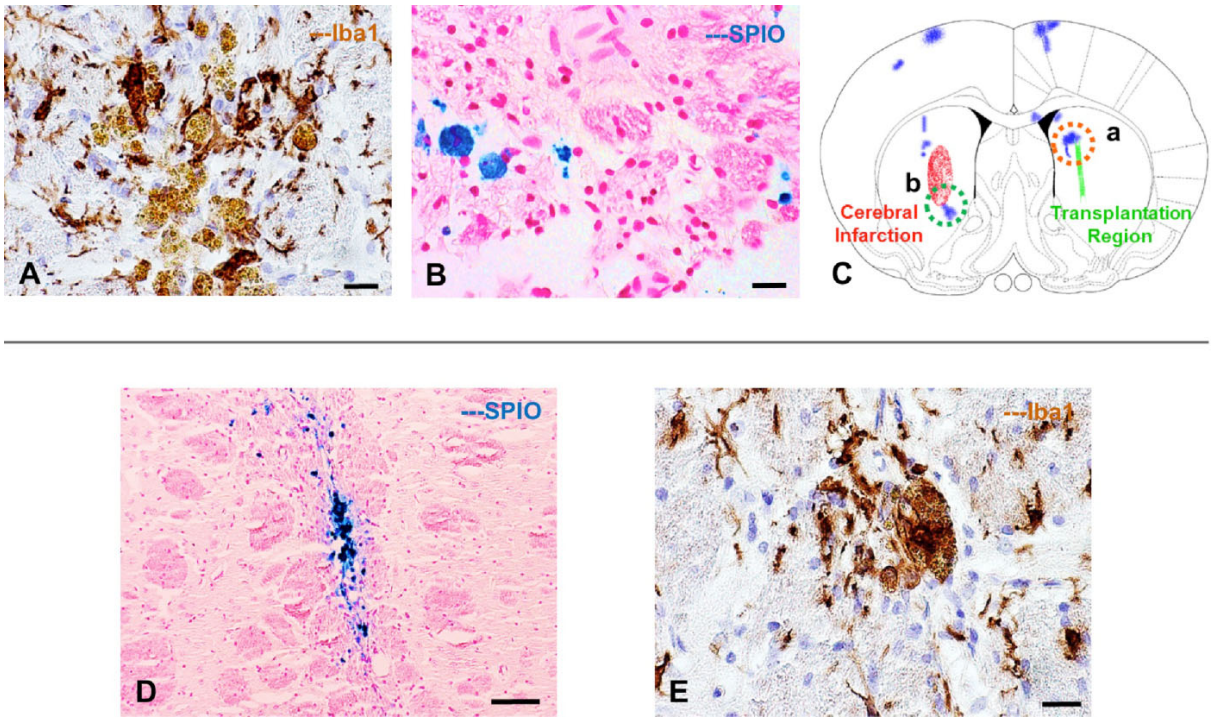

Figure 14: Immunohistochemical analysis and Turnbull blue staining in the 10-month groups. Panels A and B show representative photomicrographs around the transplantation site (A) and infarct lesion (B) in the 10-month group A. Panel A shows immunohistochemistry (brown: Iba1, yellow: SPIO, and panel B shows Turnbull Blue staining (blue: SPIO). Scale bar: 20 μm. Panel C is a schematic diagram that indicates the location of the lacunar infarct (red), the distribution of SPIO-positive cells (blue), and the location of panels A and B (broken circles) in the brain of rats from 10-month group A. Panels D and E show representative photomicrographs around the transplantation site with Turnbull blue staining (D, blue: SPIO) and immunohistochemistry (E, brown: Iba1, yellow: SPIO) in the 10-month group B. Scale bars: 100 μm (D) and 20 μm (E).

DISCUSSION

In the present study, MRI and histological analysis were employed to investigate SPIO-labeled allogeneic BMSCs' short-, middle- and long-term safety after the transplantation to rat lacunar stroke model. Serial MRI indicated that the migration of SPIO-labeled BMSCs from transplantation area to lacunar infarction lesion. Histological analysis demonstrated that activated microglia were found 7 days after BMSC transplantation, although an immunosuppressive drug was used. Some SPIO-labeled BMSCs resided and started to proliferate along the injection track. In 6 weeks group, a large numbers of SPIO-labeled BMSCs had reached the lacunar infarction area via the corpus callosum. Some SPIO nanoparticles were phagocytized by microglia. In 10 months group, the number of SPIO positive cells were lower than other groups. No severe brain injury or no tumor formation was observed in any groups.

In order to make a reproducible lacunar stroke and have a persistent motor dysfunction, a Na/K-ATPase pump inhibitor ouabain was employed[54,71]. Ouabain, the effect of which is based on membrane depolarization of excitable cells, can blockade energy-dependent ionic pump and brings metabolic and structural changes in brain. These changes have been verified to have the same pattern and development trajectory compared with focal ischemia[72]. Furthermore, the animal models which had Ouabain-induced lacunar stroke by stereotactic injection were also reported previously[54,3].

Recent studies have strongly suggested that when transplanted in cerebral ischemia models, the BMSCs could regenerate the lost neurologic function through neural differentiation, neurotrophic factor release, cell fusion adjacent the lesion, or migrate into subventricular zone (SVZ) to enhance intrinsic neurogenesis[73,22,74,75].

In the present study, a stereotactic BMSC transplantation was performed to the lacunar stroke model[76,77,3] and cell labeling with SPIO was employed to track the donor cells in host brain by means of MRI. The cultured BMSCs can take SPIO nanoparticles into their cytoplasm by the addition into culture medium. Because SPIO nanoparticles have clearly detectable signal extinction, SPIO-labeled cells are easily tracked anatomically with T2-weighted images[31].

To evaluate the safety of SPIO-labeled BMSCs histologically, immunohistochemistry with Turnbull blue staining technique was quite useful to grasp the behaviors of donor cells and to

investigate the relationship among BMSCs, ischemic brain tissue, and inflammation with microglia. The staining also showed that some SPIO-positive cells were phagocytizing microglia. As SPIO-labeled BMSC transplantation, the residual SPIO nanoparticles in vehicle might be also taken into the brains. In contrast, if SPIO-labeled BMSCs were dead, SPIO nanoparticles may be released into the brain and their deposition may be formed in tissues. Some of them were phagocytized by microglia, which were activated to phagocytize the damage cells and foreign matters. In 10 months group, SPIO-solution or SPIO-labeled BMSCs caused no severe inflammation in host brain, regardless of the presence of lacunar infarction. Unfortunately, MRI was unable to distinguish microglia phagocytizing SPIO nanoparticles from SPIO-labeled BMSCs. This is a limitation of the cell tracking method with SPIO.

With the proliferation, differentiation and migration of BMSCs, SPIO nanoparticles could move to the region where BMSCs have reached. Yano et al. reported a quite different result between SPIO-labeled BMSCs and GFP-labeled BMSCs. SPIO-positive cells did not decrease in appearance because of the distribution of SPIO nanoparticles during BMSC proliferation, but GFP-labeled BMSCs increased in terms of equal inheritance of their phenotype[78]. Because some GFP-positive and SPIO-negative BMSCs were found in transplanted cell bolus, excellent cell proliferation may have occurred in 7 days group. However, we found no tumor formation in any animals for 10 months.

It is generally accepted that microglia spread throughout anywhere and are key modulators of the immune response for noxious agents and injurious processes in the CNS[79,80]. Resting microglia display a ramified appearance, they become amoeboid and are indistinguishable from macrophages and circulating monocytes when they are activated[81]. Activated microglia have M1 and M2 major phenotypes, which are the two polars of microglial activation states in CNS[82]. Proinflammatory cytokine interferon gamma (IFN-γ) and lipopolysaccharide (LPS) promote M1 phenotype, which produces high levels of proinflammatory cytokines and oxidative metabolites to act in tissue defense and to promote the destruction of invaders[81]. In contrast, M2 microglia execute an anti-inflammatory effect and promote wound healing and tissue repair[83]. In the present study, we confirmed that M1 was the major phenotype of microglia around the injury area in the 7-day group, regardless of immunosuppression. As time passed,

the activated microglia, especial M1 phenotype, became less and less around the donor cells. This phenomenon suggested that M2 microglia would become the main phenotype gradually, instead of M1 microglia, to promote the repair and regeneration of brain lesion after acute injury period. Recently, the allogeneic BMSCs attracted a lot of attention as a cell source for clinical applications[23]. Our present results support the possible clinical utility of the allogeneic BMSC transplantation.

In addition, we found several SPIO-positive cells existed near the blood vessels. Some cells were engulfed by microglia and others were not. In recent studies, some parenchymal microglia called "juxtavascular microglia" were observed to be rapidly activated and can be preferentially recruited to the surfaces of blood vessels following brain tissue injury[84]. On the other hand, BMSCs also have been showed to have the potential to differentiate into endothelial cells and smooth muscle cells which are the major components of blood vessels[85-87]. We believed that some SPIO-positive cells were BMSCs that participated in the injury of blood vessels, and some SPIO-positive cells represented phagocytizing microglia traveling to the injury area through the blood vessels.

Summary and Conclusion

BMSCs can be harvested and cultured easily and have a great potential as cell sources of transplantation therapy for ischemic stroke. Now we are preparing a new phase 1 clinical trial called the RAINBOW study for acute ischemic stroke patients. In the present study, BMSCs were cultured with allogeneic PL, labeled by SPIO, and stereotactically transplanted into animals' brains as presented in Chapter 1 and 2 and obtained the following results to be applied to the clinical therapy.

1. Using ELISA analysis, we found that platelet cell surface antigens (CD61 and CD41) cannot be detected in the 10% PL-supplemented culture medium. Flow cytometric analysis didn't find any mutation of BMSCs after being cultured by PL-supplemented medium. This finding demonstrated that PL products is safety for clinical application.
2. The contents of growth factors (PDGF-BB, TGF-β1 and BDNF) in PL are adequate for cell culture. When the contents of platelets in original PC reached more than 15 units, the cell proliferating potential of PL was equivalent or much higher compared with the FCS.
3. SPIO labeled BMSCs can be detected easily by MRI. In the 3-week after transplantation, MRI showed low signal intensity in the corpus callosum and right external capsule. This suggested that SPIO-BMSCs may start to migrate through the corpus callosum to the infarction region.
4. In histology, from 7-day group to 10-month groups, none of animals were observed to develop either a tumor or severe inflammation. And the BMSCs which expressed NeuN were found around the infarction lesion. This exhibited that SPIO-BMSCs have the same differentiating ability as normal BMSCs.

These finding not only demonstrate that BMSCs with allogeneic PL-supplement may be valuable, feasible, safe and effectible for cell therapy against ischemic stroke but also provide a new way for avoiding zoonoses and monitoring the transplanted cells. The RAINBOW study will start on Feb 2017, we will translate these results to the protocol of RAINBOW, and we hope that it will be helpful for the patients who suffer from stroke.

Acknowledgments

I would like to express my deepest gratitude to my Professor Kiyohiro Houkin, the head of Department of Neurosurgery, Hokkaido University Graduate School of Medicine, for giving me the opportunity to study as a doctoral course student. It is my honor to be his student.

Mostly I want to express my great appreciation to my supervisor Professor Hideo Shichinohe, who supported my research, gave a widely space to make me explore my own research idea, and took care of my life in the past 4 years. Without his trust, encouragement, and help, I couldn't smoothly complete my doctoral career.

I also want to express my sincere gratitude to professor Yuji Kuge from Central Institute of Isotope Science Hokkaido University, professor Songji Zhao from Advanced Clinical Research Center and Fukushima Global Medical Science Center Fukushima Medical University, professor Tsuneo Ito from Hokkaido University Hospital Clinical Research and Medical Innovation Center, professor Kohsuke Kudo from Department of Radiology Hokkaido University, and professor Shigeru Takamoto from Japanese Red Cross Hokkaido Block Blood Center. They provided a huge support for my research.

I would like to thank research associate Mrs. Rika Nagashima and secretary Miss Mika Murakami. They taught me a lot of knowledge and encourage me every day. With their help, I had courage to achieve one goal after another.

All members in the Department of Neurosurgery of Hokkaido University have contributed immensely to my life in Japan. Thank you all for accompany me in the past four years.

Thank and mourn for all animals which sacrificed during research.

Thanks a lot to Hokkaido University for giving me the tuition fees exemption. Thanks a lot to Japanese Government, Top Global University Project, Otsuka Toshimi Scholarship Foundation, and OTOWA HIROTSUGU scholarship for giving me the foundation. Thanks a lot to SENSHIN Medical Research Foundation for supporting my research.

At last, I want to express my deep appreciation to my family and friends for providing huge supports and encouragements for me.

References

1 Donnan, G. A., Fisher, M., Macleod, M. & Davis, S. M. Stroke. *Lancet* **371**, 1612-1623 (2008).

2 Murray, C. J. & Lopez, A. D. Mortality by cause for eight regions of the world: Global Burden of Disease Study. *Lancet* **349**, 1269-1276 (1997).

3 Shichinohe, H., Yamauchi, T., Saito, H., Houkin, K. & Kuroda, S. Bone marrow stromal cell transplantation enhances recovery of motor function after lacunar stroke in rats. *Acta Neurobiol. Exp. (Wars.)* **73**, 354-363 (2013).

4 Bliss, T., Guzman, R., Daadi, M. & Steinberg, G. K. Cell transplantation therapy for stroke. *Stroke* **38**, 817-826 (2007).

5 Kuroda, S., Shichinohe, H., Houkin, K. & Iwasaki, Y. Autologous bone marrow stromal cell transplantation for central nervous system disorders - recent progress and perspective for clinical application. *J. Stem Cells Regen. Med.* **7**, 2-13 (2011).

6 Parr, A. M., Tator, C. H. & Keating, A. Bone marrow-derived mesenchymal stromal cells for the repair of central nervous system injury. *Bone Marrow Transplant.* **40**, 609-619 (2007).

7 Chen, J., Li, Y., Wang, L., Lu, M., Zhang, X. & Chopp, M. Therapeutic benefit of intracerebral transplantation of bone marrow stromal cells after cerebral ischemia in rats. *J. Neurol. Sci.* **189**, 49-57 (2001).

8 Chen, J., Li, Y., Wang, L., Zhang, Z., Lu, D., Lu, M. & Chopp, M. Therapeutic benefit of intravenous administration of bone marrow stromal cells after cerebral ischemia in rats. *Stroke* **32**, 1005-1011 (2001).

9 Sugiyama, T., Kuroda, S., Takeda, Y., Nishio, M., Ito, M., Shichinohe, H. & Koike, T. Therapeutic impact of human bone marrow stromal cells expanded by animal serum-free medium for cerebral infarct in rats. *Neurosurgery* **68**, 1733-1742; discussion 1742 (2011).

10 Brighton, C. T. & Hunt, R. M. Early histologic and ultrastructural changes in microvessels of periosteal callus. *J. Orthop. Trauma* **11**, 244-253 (1997).

11 Oni, O. O. Early histological and ultrastructural changes in medullary fracture callus. *J. Bone Joint Surg. Am.* **74**, 633-634 (1992).

12 Pittenger, M. F., Mackay, A. M., Beck, S. C., Jaiswal, R. K., Douglas, R., Mosca, J. D., Moorman, M. A., Simonetti, D. W., Craig, S. & Marshak, D. R. Multilineage potential of adult human mesenchymal stem cells. *Science* **284**, 143-147 (1999).

13 Azizi, S. A., Stokes, D., Augelli, B. J., DiGirolamo, C. & Prockop, D. J. Engraftment and migration of human bone marrow stromal cells implanted in the brains of albino rats--similarities to astrocyte grafts. *Proc. Natl. Acad. Sci. U. S. A.* **95**, 3908-3913 (1998).

14 Kopen, G. C., Prockop, D. J. & Phinney, D. G. Marrow stromal cells migrate throughout forebrain and cerebellum, and they differentiate into astrocytes after injection into neonatal mouse brains. *Proc. Natl. Acad. Sci. U. S. A.* **96**, 10711-10716 (1999).

15 Sanchez-Ramos, J., Song, S., Cardozo-Pelaez, F., Hazzi, C., Stedeford, T., Willing, A., Freeman, T. B., Saporta, S., Janssen, W., Patel, N., Cooper, D. R. & Sanberg, P. R. Adult bone marrow stromal cells differentiate into neural cells in vitro. *Exp. Neurol.* **164**, 247-256 (2000).

16 Woodbury, D., Schwarz, E. J., Prockop, D. J. & Black, I. B. Adult rat and human bone marrow stromal cells differentiate into neurons. *J. Neurosci. Res.* **61**, 364-370 (2000).

17 Yamaguchi, S., Kuroda, S., Kobayashi, H., Shichinohe, H., Yano, S., Hida, K., Shinpo, K., Kikuchi, S. & Iwasaki, Y. The effects of neuronal induction on gene expression profile in bone marrow stromal cells (BMSC)--a preliminary study using microarray analysis. *Brain Res.* **1087**, 15-27 (2006).

18 Chen, Q., Long, Y., Yuan, X., Zou, L., Sun, J., Chen, S., Perez-Polo, J. R. & Yang, K. Protective effects of bone marrow stromal cell transplantation in injured rodent brain: synthesis of neurotrophic factors. *J. Neurosci. Res.* **80**, 611-619 (2005).

19 Chopp, M. & Li, Y. Treatment of neural injury with marrow stromal cells. *Lancet Neurol.* **1**, 92-100 (2002).

20 Garcia, R., Aguiar, J., Alberti, E., de la Cuetara, K. & Pavon, N. Bone marrow stromal cells produce nerve growth factor and glial cell line-derived neurotrophic factors. *Biochem. Biophys. Res. Commun.* **316**, 753-754 (2004).

21 He, X. Y., Chen, Z. Z., Cai, Y. Q., Xu, G., Shang, J. H., Kou, S. B., Li, M., Zhang, H. T., Duan, C. Z., Zhang, S. Z., Ke, Y. Q., Zeng, Y. J., Xu, R. X. & Jiang, X. D. Expression of cytokines in rat brain with focal cerebral ischemia after grafting with bone marrow stromal cells and endothelial progenitor cells. *Cytotherapy* **13**, 46-53 (2011).

22 Hokari, M., Kuroda, S., Shichinohe, H., Yano, S., Hida, K. & Iwasaki, Y. Bone marrow stromal cells protect and repair damaged neurons through multiple mechanisms. *J. Neurosci. Res.* **86**, 1024-1035 (2008).

23 Savitz, S. I., Chopp, M., Deans, R., Carmichael, T., Phinney, D., Wechsler, L. & Participants, S. Stem Cell Therapy as an Emerging Paradigm for Stroke (STEPS) II. *Stroke* **42**, 825-829 (2011).

24 Shichinohe, H., Ishihara, T., Takahashi, K., Tanaka, Y., Miyamoto, M., Yamauchi, T., Saito, H., Takemoto, H., Houkin, K. & Kuroda, S. Bone marrow stromal cells rescue ischemic brain by trophic effects and phenotypic change toward neural cells. *Neurorehabil. Neural Repair* **29**, 80-89 (2015).

25 Zhong, C., Qin, Z., Zhong, C. J., Wang, Y. & Shen, X. Y. Neuroprotective effects of bone marrow stromal cells on rat organotypic hippocampal slice culture model of cerebral ischemia. *Neurosci. Lett.* **342**, 93-96 (2003).

26 Shichinohe, H. & Houkin, K. Cell Therapy for Stroke: Review of Previous Clinical Trials and Introduction of Our New Trials. *Neurol. Med. Chir. (Tokyo)* **56**, 592-596 (2016).

27 Bang, O. Y., Lee, J. S., Lee, P. H. & Lee, G. Autologous mesenchymal stem cell transplantation in stroke patients. *Ann. Neurol.* **57**, 874-882 (2005).

28 Kuroda, S., Shichinohe, H., Houkin, K., K, H. & Iwasaki, Y. Autologous bone marrow stromal cell transplantation for central nervous system disorders - recent progress and perspective for clinical application. *J. Stem Cells Regen. Med.* **7**, 2-13 (2011).

29 Fekete, N., Gadelorge, M., Furst, D., Maurer, C., Dausend, J., Fleury-Cappellesso, S., Mailander, V., Lotfi, R., Ignatius, A., Sensebe, L., Bourin, P., Schrezenmeier, H. & Rojewski, M. T. Platelet lysate from whole blood-derived pooled platelet concentrates and apheresis-derived platelet concentrates for the isolation and expansion of human bone marrow mesenchymal stromal cells: production process, content and identification of active components. *Cytotherapy* **14**, 540-554 (2012).

30 Mannello, F. & Tonti, G. A. Concise review: no breakthroughs for human mesenchymal and embryonic stem cell culture: conditioned medium, feeder layer, or feeder-free; medium with fetal calf serum, human serum, or enriched plasma; serum-free, serum replacement nonconditioned medium, or ad hoc formula? All that glitters is not gold! *Stem Cells* **25**, 1603-1609 (2007).

31 Shichinohe, H., Kuroda, S., Kudo, K., Ito, M., Kawabori, M., Miyamoto, M., Nakanishi, M., Terae, S. & Houkin, K. Visualization of the Superparamagnetic Iron Oxide (SPIO)-Labeled Bone Marrow Stromal Cells Using a 3.0-T MRI-a Pilot Study for Clinical Testing of Neurotransplantation. *Transl Stroke Res.* **3**, 99-106 (2012).

32 Sotiropoulou, P. A., Perez, S. A., Salagianni, M., Baxevanis, C. N. & Papamichail, M. Characterization of the optimal culture conditions for clinical scale production of human mesenchymal stem cells. *Stem Cells* **24**, 462-471 (2006).

33 Sugiyama, T., Kuroda, S., Osanai, T., Shichinohe, H., Kuge, Y., Ito, M., Kawabori, M. & Iwasaki, Y. Near-infrared fluorescence labeling allows noninvasive tracking of bone marrow stromal cells transplanted into rat infarct brain. *Neurosurgery* **68**, 1036-1047; discussion 1047 (2011).

34 Reinhardt, J., Stuhler, A. & Blumel, J. Safety of bovine sera for production of mesenchymal stem cells for therapeutic use. *Hum. Gene Ther.* **22**, 775; author reply 776 (2011).

35 Sensebe, L., Bourin, P. & Tarte, K. Good manufacturing practices production of mesenchymal stem/stromal cells. *Hum. Gene Ther.* **22**, 19-26 (2011).

36 Wu, R. X., Yu, Y., Yin, Y., Zhang, X. Y., Gao, L. N. & Chen, F. M. Platelet lysate supports the in vitro expansion of human periodontal ligament stem cells for cytotherapeutic use. *J. Tissue Eng. Regen. Med.* (2016).

37 Horn, P., Bokermann, G., Cholewa, D., Bork, S., Walenda, T., Koch, C., Drescher, W., Hutschenreuther, G., Zenke, M., Ho, A. D. & Wagner, W. Impact of individual platelet lysates on isolation and growth of human mesenchymal stromal cells. *Cytotherapy* **12**, 888-898 (2010).

38 Shichinohe, H., Kuroda, S., Sugiyama, T., Ito, M., Kawabori, M., Nishio, M., Takeda, Y., Koike, T. & Houkin, K. Biological Features of Human Bone Marrow Stromal Cells (hBMSC) Cultured with Animal Protein-Free Medium-Safety and Efficacy of Clinical Use for Neurotransplantation. *Transl Stroke Res.* **2**, 307-315 (2011).

39 Heiskanen, A., Satomaa, T., Tiitinen, S., Laitinen, A., Mannelin, S., Impola, U., Mikkola, M., Olsson, C., Miller-Podraza, H., Blomqvist, M., Olonen, A., Salo, H., Lehenkari, P., Tuuri, T., Otonkoski, T., Natunen, J., Saarinen, J. & Laine, J. N-glycolylneuraminic acid xenoantigen contamination of human embryonic and mesenchymal stem cells is substantially reversible. *Stem Cells* **25**, 197-202 (2007).

40 Sundin, M., Ringden, O., Sundberg, B., Nava, S., Gotherstrom, C. & Le Blanc, K. No alloantibodies against mesenchymal stromal cells, but presence of anti-fetal calf serum antibodies, after transplantation in allogeneic hematopoietic stem cell recipients. *Haematologica* **92**, 1208-1215 (2007).

41 Chen, F. M. & Liu, X. Advancing biomaterials of human origin for tissue engineering. *Prog Polym Sci* **53**, 86-168 (2016).

42 Stute, N., Holtz, K., Bubenheim, M., Lange, C., Blake, F. & Zander, A. R. Autologous serum for isolation and expansion of human mesenchymal stem cells for clinical use. *Exp. Hematol.* **32**, 1212-1225 (2004).

43 Tchang, L. A., Pippenger, B. E., Todorov, A., Jr., Wolf, F., Burger, M. G., Jaquiery, C., Bieback, K., Martin, I., Schaefer, D. J. & Scherberich, A. Pooled thrombin-activated platelet-rich plasma: a substitute for fetal bovine serum in the engineering of osteogenic/vasculogenic grafts. *J. Tissue Eng. Regen. Med.* (2015).

44 Burnouf, T., Strunk, D., Koh, M. B. & Schallmoser, K. Human platelet lysate: Replacing fetal bovine serum as a gold standard for human cell propagation? *Biomaterials* **76**, 371-387 (2016).

45 Hara, Y., Steiner, M. & Baldini, M. G. Platelets as a source of growth-promoting factor(s) for tumor cells. *Cancer Res.* **40**, 1212-1216 (1980).

46 Ploderl, K., Strasser, C., Hennerbichler, S., Peterbauer-Scherb, A. & Gabriel, C. Development and validation of a production process of platelet lysate for autologous use. *Platelets* **22**, 204-209 (2011).

47 Yamauchi, T., Saito, H., Ito, M., Shichinohe, H., Houkin, K. & Kuroda, S. Platelet lysate and granulocyte-colony stimulating factor serve safe and accelerated expansion of human bone marrow stromal cells for stroke therapy. *Transl Stroke Res.* **5**, 701-710 (2014).

48 Bernardo, M. E., Avanzini, M. A., Perotti, C., Cometa, A. M., Moretta, A., Lenta, E., Del Fante, C., Novara, F., de Silvestri, A., Amendola, G., Zuffardi, O., Maccario, R. & Locatelli, F. Optimization of in vitro expansion of human multipotent mesenchymal stromal cells for cell-therapy approaches: Further insights in the search for a fetal calf serum substitute. *J. Cell. Physiol.* **211**, 121-130 (2007).

49 Doucet, C., Ernou, I., Zhang, Y., Llense, J. R., Begot, L., Holy, X. & Lataillade, J. J. Platelet lysates promote

mesenchymal stem cell expansion: a safety substitute for animal serum in cell-based therapy applications. *J. Cell. Physiol.* **205**, 228-236 (2005).

50 Eppley, B. L., Woodell, J. E. & Higgins, J. Platelet quantification and growth factor analysis from platelet-rich plasma: implications for wound healing. *Plast. Reconstr. Surg.* **114**, 1502-1508 (2004).

51 Ben Azouna, N., Jenhani, F., Regaya, Z., Berraeis, L., Ben Othman, T., Ducrocq, E. & Domenech, J. Phenotypical and functional characteristics of mesenchymal stem cells from bone marrow: comparison of culture using different media supplemented with human platelet lysate or fetal bovine serum. *Stem Cell. Res. Ther.* **3**, 6 (2012).

52 Perez-Ilzarbe, M., Diez-Campelo, M., Aranda, P., Tabera, S., Lopez, T., del Canizo, C., Merino, J., Moreno, C., Andreu, E. J., Prosper, F. & Perez-Simon, J. A. Comparison of ex vivo expansion culture conditions of mesenchymal stem cells for human cell therapy. *Transfusion (Paris)* **49**, 1901-1910 (2009).

53 Schallmoser, K., Bartmann, C., Rohde, E., Reinisch, A., Kashofer, K., Stadelmeyer, E., Drexler, C., Lanzer, G., Linkesch, W. & Strunk, D. Human platelet lysate can replace fetal bovine serum for clinical-scale expansion of functional mesenchymal stromal cells. *Transfusion (Paris)* **47**, 1436-1446 (2007).

54 Janowski, M., Gornicka-Pawlak, E., Kozlowska, H., Domanska-Janik, K., Gielecki, J. & Lukomska, B. Structural and functional characteristic of a model for deep-seated lacunar infarct in rats. *J. Neurol. Sci.* **273**, 40-48 (2008).

55 Cho, H. S., Song, I. H., Park, S. Y., Sung, M. C., Ahn, M. W. & Song, K. E. Individual variation in growth factor concentrations in platelet-rich plasma and its influence on human mesenchymal stem cells. *Korean J. Lab. Med.* **31**, 212-218 (2011).

56 Donovan, J., Abraham, D. & Norman, J. Platelet-derived growth factor signaling in mesenchymal cells. *Front. Biosci. (Landmark Ed.)* **18**, 106-119 (2013).

57 Kikuchi, K., Soma, Y., Fujimoto, M., Kadono, T., Sato, S., Abe, M., Ohhara, K. & Takehara, K. Dermatofibrosarcoma protuberans: increased growth response to platelet-derived growth factor BB in cell culture. *Biochem. Biophys. Res. Commun.* **196**, 409-415 (1993).

58 Devescovi, V., Leonardi, E., Ciapetti, G. & Cenni, E. Growth factors in bone repair. *Chir. Organi Mov.* **92**, 161-168 (2008).

59 Adesida, A. B., Mulet-Sierra, A. & Jomha, N. M. Hypoxia mediated isolation and expansion enhances the chondrogenic capacity of bone marrow mesenchymal stromal cells. *Stem Cell. Res. Ther.* **3**, 9 (2012).

60 Fukiage, K., Aoyama, T., Shibata, K. R., Otsuka, S., Furu, M., Kohno, Y., Ito, K., Jin, Y., Fujita, S., Fujibayashi, S., Neo, M., Nakayama, T., Nakamura, T. & Toguchida, J. Expression of vascular cell adhesion molecule-1 indicates the differentiation potential of human bone marrow stromal cells. *Biochem. Biophys. Res. Commun.* **365**, 406-412 (2008).

61 Vishwakarma, A., Sharpe, P., Shi, S. & Ramalingam, M. *Stem Cell Biology and Tissue Engineering in Dental Sciences*. (Academic Press, 2014).

62 Tan, C., Shichinohe, H., Abumiya, T., Nakayama, N., Kazumata, K., Hokari, M., Hamauchi, S. & Houkin, K. Short-, middle- and long-term safety of superparamagnetic iron oxide-labeled allogeneic bone marrow stromal cell transplantation in rat model of lacunar infarction. *Neuropathology* **35**, 197-208 (2015).

63 Garcon, G., Garry, S., Gosset, P., Zerimech, F., Martin, A., Hannothiaux, M. & Shirali, P. Benzo(a)pyrene-coated onto Fe(2)O(3) particles-induced lung tissue injury: role of free radicals. *Cancer Lett.* **167**, 7-15 (2001).

64 He, T., Wang, Y., Xiang, J. & Zhang, H. In Vivo Tracking of Novel SPIO-Molday ION Rhodamine-B-Labeled Human Bone Marrow-Derived Mesenchymal Stem Cells After Lentivirus- Mediated COX-2 Silencing: A Preliminary Study. *Curr. Gene Ther.* **14**, 136-145 (2014).

65 Kraitchman, D. L., Heldman, A. W., Atalar, E., Amado, L. C., Martin, B. J., Pittenger, M. F., Hare, J. M. & Bulte, J. W. In vivo magnetic resonance imaging of mesenchymal stem cells in myocardial infarction. *Circulation* **107**, 2290-2293 (2003).

66 Xu, H. S., Ma, C., Cao, L., Wang, J. J. & Fan, X. X. Study of co-transplantation of SPIO labeled bone marrow stromal stem cells and Schwann cells for treating traumatic brain injury in rats and in vivo tracing of magnetically labeled cells by MRI. *Eur. Rev. Med. Pharmacol. Sci.* **18**, 520-525 (2014).

67 Zhao, S., Wang, Y., Gao, C., Zhang, J., Bao, H., Wang, Z. & Gong, P. Superparamagnetic iron oxide magnetic nanomaterial-labeled bone marrow mesenchymal stem cells for rat liver repair after hepatectomy. *J. Surg. Res.* (2014).

68 Taylor, A., Wilson, K. M., Murray, P., Fernig, D. G. & Levy, R. Long-term tracking of cells using inorganic nanoparticles as contrast agents: are we there yet? *Chem. Soc. Rev.* **41**, 2707-2717 (2012).

69 Wang, Y. X. Superparamagnetic iron oxide based MRI contrast agents: Current status of clinical application. *Quant Imaging Med Surg* **1**, 35-40 (2011).

70 Ito, M., Kuroda, S., Sugiyama, T., Shichinohe, H., Takeda, Y., Nishio, M., Koike, T. & Houkin, K. Validity of bone marrow stromal cell expansion by animal serum-free medium for cell transplantation therapy of cerebral infarct in rats-a serial MRI study. *Transl Stroke Res.* **2**, 294-306 (2011).

71 van der Stelt, M., Veldhuis, W. B., van Haaften, G. W., Fezza, F., Bisogno, T., Bar, P. R., Veldink, G. A., Vliegenthart, J. F., Di Marzo, V. & Nicolay, K. Exogenous anandamide protects rat brain against acute neuronal injury in vivo. *J. Neurosci.* **21**, 8765-8771 (2001).

72 Veldhuis, W. B., van der Stelt, M., Delmas, F., Gillet, B., Veldink, G. A., Vliegenthart, J. F., Nicolay, K. & Bar, P. R. In vivo excitotoxicity induced by ouabain, a Na+/K+-ATPase inhibitor. *J. Cereb. Blood Flow Metab.* **23**, 62-74 (2003).

73 Alvarez-Buylla, A., Garcia-Verdugo, J. M. & Tramontin, A. D. A unified hypothesis on the lineage of neural stem cells. *Nat. Rev. Neurosci.* **2**, 287-293 (2001).

74 Kuroda, S. Bone marrow stromal cell transplantation for ischemic stroke -- its multi-functional feature. *Acta Neurobiol. Exp. (Wars.)* **73**, 57-65 (2013).

75 Zhang, R. L., Zhang, Z. G. & Chopp, M. Ischemic stroke and neurogenesis in the subventricular zone. *Neuropharmacology* **55**, 345-352 (2008).

76 Kawabori, M., Kuroda, S., Ito, M., Shichinohe, H., Houkin, K., Kuge, Y. & Tamaki, N. Timing and cell dose determine therapeutic effects of bone marrow stromal cell transplantation in rat model of cerebral infarct. *Neuropathology* **33**, 140-148 (2013).

77 Miyamoto, M., Kuroda, S., Zhao, S., Magota, K., Shichinohe, H., Houkin, K., Kuge, Y. & Tamaki, N. Bone marrow stromal cell transplantation enhances recovery of local glucose metabolism after cerebral infarction in rats: a serial 18F-FDG PET study. *J. Nucl. Med.* **54**, 145-150 (2013).

78 Yano, S., Kuroda, S., Shichinohe, H., Hida, K. & Iwasaki, Y. Do bone marrow stromal cells proliferate after transplantation into mice cerebral infarct?--a double labeling study. *Brain Res.* **1065**, 60-67 (2005).

79 Kreutzberg, G. W. Microglia: a sensor for pathological events in the CNS. *Trends Neurosci.* **19**, 312-318 (1996).

80 Nimmerjahn, A., Kirchhoff, F. & Helmchen, F. Resting microglial cells are highly dynamic surveillants of brain parenchyma in vivo. *Science* **308**, 1314-1318 (2005).

81 Kawabori, M. & Yenari, M. A. The role of the microglia in acute CNS injury. *Metab. Brain Dis.* (2014).

82 Tang, Y., Li, T., Li, J., Yang, J., Liu, H., Zhang, X. J. & Le, W. Jmjd3 is essential for the epigenetic modulation of microglia phenotypes in the immune pathogenesis of Parkinson's disease. *Cell Death Differ.* **21**, 369-380 (2014).

83 Gordon, S. Alternative activation of macrophages. *Nat. Rev. Immunol.* **3**, 23-35 (2003).

84 Grossmann, R., Stence, N., Carr, J., Fuller, L., Waite, M. & Dailey, M. E. Juxtavascular microglia migrate along brain microvessels following activation during early postnatal development. *Glia* **37**, 229-240 (2002).

85 Liu, J. W., Dunoyer-Geindre, S., Serre-Beinier, V., Mai, G., Lambert, J. F., Fish, R. J., Pernod, G., Buehler, L., Bounameaux, H. & Kruithof, E. K. Characterization of endothelial-like cells derived from human mesenchymal stem cells. *J. Thromb. Haemost.* **5**, 826-834 (2007).

86 Tamama, K., Sen, C. K. & Wells, A. Differentiation of bone marrow mesenchymal stem cells into the smooth muscle lineage by blocking ERK/MAPK signaling pathway. *Stem Cells Dev.* **17**, 897-908 (2008).

87 Zhen-Zhou, C., Xiao-Dan, J., Gui-Tao, L., Jiang-Hua, S., Ling-Hui, L., Mou-Xuan, D. & Ru-Xiang, X. Functional and ultrastructural analysis of endothelial-like cells derived from bone marrow stromal cells. *Cytotherapy* **10**, 611-624 (2008).